SOME PHYSICAL AND STATISTICAL STUDIES OF METEOR FRAGMENTATION

Richard Eugene McCrosky

(3)

SOME PHYSICAL AND STATISTICAL STUDIES OF METEOR FRAGMENTATION

A thesis presented

by

Richard Eugene McCrosky

to

The Astronomy Department

in partial fulfillment of the requirements

for the degree of

Doctor of Philosophy

in the subject of

Astronomy

Harvard University

Cambridge, Massachusetts

November, 1955

ACKNOWLEDGEMENTS

Any scientific endeavor that can be attributed to a single person is a rare phenomenon and perhaps a thesis, in many ways the end product of the labors of one's teachers, represents the ultimate in cooperative research. In this respect I have been exceptionally fortunate in having the opportunity to study under the Council and staff members of the Harvard College Observatory. I wish to express my gratitude to them.

I am indebted to all of the members of the Harvard Meteor Project in New Mexico for the acquisition of the photographic data and to the Project staff in Cambridge for the time and thought they have given in discussing the various problems of this work. I wish particularly to thank Dr. Luigi G. Jacchia for the ready access he has given to the results of his reductions obtained under Office of Ordnance Research Contract No. DA-19-020-ORD-2556.

The problem was suggested by Dr. Fred L. Whipple. For his advice in this specific example and the inspiration he has given during my years as a student I am in great debt, and to an even greater extent, to Dr. Whipple and to Dr. Richard N. Thomas for the encouragement and pleasant insistences that were responsible for the continuation of my education.

To my wife, Jean, go my special thanks for the assistance and support, both material and otherwise, she has given when it was most needed.

I am grateful to Mrs. Lyle Boyd for editing the text and to Mrs. Lillian Battle Christmas for preparing the final manuscript.

Finally, it is a pleasure to acknowledge the support of the Office of Naval Research. Essentially all of this work was performed under Contract No. N5ori-07647. The photographic material was acquired with the support of the ONR, Air Force Contract No. AF19(122)-482, and Naval Ordnance Contract No. NOrd 10449.

DEFINITIONS

Because the terminology in the field of meteor astronomy has sometimes been confusing it seems advisable to present the definitions of some words and phrases as they will be used here.

Both meteor and meteoroid are used to designate the body producing the meteoric phenomena although, strictly speaking, a meteor is a phenomenon and a meteoroid is the body that produces it. This duplication of terms is not a necessity but it is customary; habit is our only excuse for using both. Meteoroid is usually reserved for discussions of the physical or chemical properties of the material itself. Meteor, on the other hand, often indicates our concern with the kinematics of the body. Thus, we refer to the density of the meteoroid and to the velocity of the meteor.

A photograph of a meteor is called a trail. The trail appears on the photographic film as a series of dashes (exposed portion) and breaks (unexposed portion caused by an occulting shutter). One shutter cycle is the distance, in space or time, covered by a dash and a break. A meteor photographed by two cameras at different stations is a meteor pair. If photographed by one camera only, the trail is called a single-station meteor.

When observing a bright meteor visually, one often sees a streak of luminosity, after the passage of the meteor, which may persist for a matter of seconds. This delayed luminosity is referred to as the meteor train. Presumably it is caused by recombinations of meteoric and atmospheric ions and atoms. If a train-producing meteor were photographed, the effect of the train would be to fill in the breaks of the trail. The same kind of result would be seen on a meteor photograph if small particles were detached from the meteoroid. These fragmented particles would decelerate with respect to the larger body and, eventually, lag behind. The luminosity derived from the fragments would, in part, fall in the breaks of the trail produced by the meteor itself. We will refer to this phenomenon as the meteor wake. A part of this thesis will be an attempt to show that the above definition serves as a reasonable interpretation of most of the intensity in the breaks. It will be convenient to assume, for the present, that the preceeding explanation is correct. The justification will be presented (Chapter IV) when sufficient data are available.

If the meteoroid breaks into many particles of about the same size, the slight differential deceleration may eventually cause the luminosity to extend over an appreciable length of the trail. In such a case the breaks may be altogether obliterated and we see a phenomenon called "blending." Since this will be observed at the end of the trail, it has been designated as terminal blending.

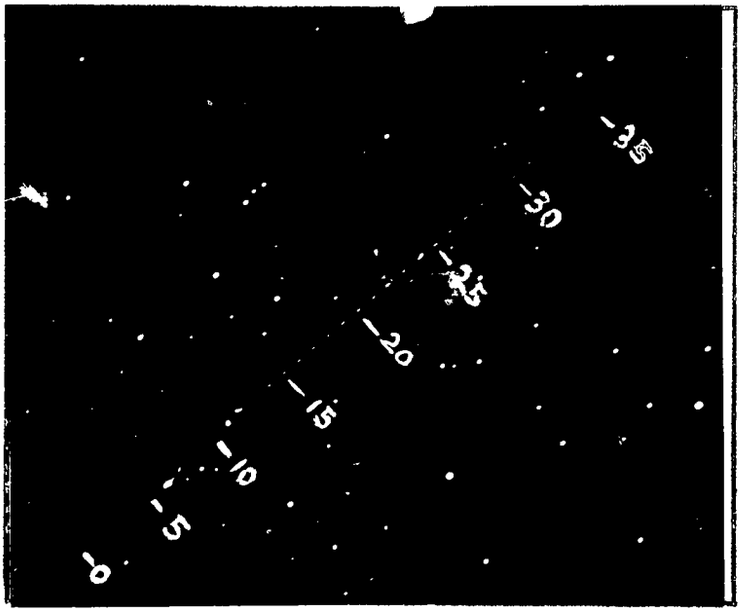

METEOR NO. 3567

An enlargement (4x) of a meteor trail showing wake and some terminal blending.

TABLE OF CONTENTS

TABLE OF CONTENTS (continued)

CHAPTER I

BACKGROUND

A. Meteor Problems

The various aspects of meteor astronomy may be described by a series of questions, not yet answered in their entirety, that might arise in the mind of any scientist confronted with the elementary observational facts. What is the origin of meteors, and their history in space? What is their physical and chemical structure? These might be called the astronomical questions. They are distinct from the physical questions: how do these bodies interact with the atmosphere, dynamically and physically? The first two questions are self-explanatory and their answers, in general, will be descriptive. The last problems are analytic in nature, and may be enlarged upon immediately.

We require that momentum and energy be conserved in any process as the meteor penetrates the atmosphere and collides with the air molecules. The rate of change of momentum is given by the drag equation:

$$m \frac{dv}{dt} = -\Gamma A(\rho v)\, v, \qquad (1)$$

where

ρ = atmospheric density,

v = meteor velocity with respect to the atmosphere,

ρv = mass of air penetrated by a unit area of the meteoroid per second,

A = effective area of the meteoroid, i.e., the frontal area projected on a plane perpendicular to the meteor's motion,

Γ = the drag coefficient, a unitless number representing, in essence, the elasticity of collisions between the air molecules and the meteoroid, and

m = mass of the meteoroid.

We may substitute for the effective area the quantity

$$A = Am^{2/3} \delta_m^{-2/3}, \tag{2}$$

where

δ_m = density of the meteoroid, and

A = a shape factor.

Then from (1) and (2) it follows that

$$\frac{dv}{dt} = -\Gamma A \delta^{-2/3} m^{-1/3} \rho v^2. \tag{3}$$

Given a knowledge of the parameters of this equation, we have then solved the dynamical problem.

With respect to the energy, we can state <u>a priori</u> that the energy per second available for all processes is:

$$\frac{dE}{dt} = \frac{1}{2} A \rho v^3. \tag{4}$$

That the collisions are not elastic is obvious from the fact that the meteor is observed; that is, some translational energy is dissipated in the form of radiation. Energy may be

dissipated through dissociation of meteoric and air molecules, excitation, ionisation, compression of air, sputtering of atoms or fragmentation of larger particles from the meteoroid surface, and heating of the meteoroid with subsequent vaporization. The rate of mass loss of the meteoroid depends on the last three of these processes: sputtering, fragmentation, and vaporization. The rate at which energy is supplied to each of these processes will be some fraction, Λ_1, of the total rate, or

$$\sum_i \frac{dE_i}{dt} = \sum_i \Lambda_i \frac{1}{2} A \rho v^3, \qquad (5)$$

where the subscript i refers to any of the various mass-loss processes. If ξ_i is the energy required to remove a gram of material by a particular process, then the mass loss is given by the equation

$$\sum_i \frac{dm_i}{dt} = -\frac{1}{2} \sum_i \frac{\Lambda_i}{\xi_i} A \rho v^3. \qquad (6a)$$

The existing data on sputtering indicates that this method of ablation will be unimportant compared to vaporization. In any case, our observations cannot distinguish between the two processes.

The second physical problem relates to the luminosity of the meteor. From the spectra of meteors we know that much of the light occurs in lines arising from electronic transitions in meteoric atoms. The black body radiation is

small, as it must be for bodies of this size at their vaporization temperature. These facts alone are sufficient to suggest that the luminosity is due to collisional excitation of ablated meteor atoms. The important theoretical problem, attacked by Öpik (1933), is the derivation of the luminosity factor, τ. This quantity relates the available energy to the amount of visible (or photographic) light produced by the meteor. We assume that the radiation is proportional to the kinetic energy, with respect to the colliding air molecules, of the ablated meteor atoms. Then, the intensity per second is given by the relation

$$I = -\frac{1}{2}\tau v^2 \frac{dm}{dt}. \qquad (7a)$$

The mass loss, $\frac{dm}{dt}$, in this equation represents only that mass lost in such a form that a later collision with an air molecule will produce light. That is, the material must be lost in atomic (or possibly molecular) form. This type of loss includes sputtering or vaporization but not fragmentation or melting with consequent loss of molten droplets. In these latter cases, the fragments or droplets must themselves be vaporized before light is produced. The actual mass loss which is measured at any time is, on the basis of Öpik's theory, an atomic particle loss. We will, then, rewrite equation (6a) in the form,

$$\dot{m} = \frac{dm}{dt} = -\frac{\Lambda}{2\zeta} A\rho v^3 = -\frac{\Lambda}{2\zeta} A\delta_m^{-2/3} m^{2/3} \rho v^3, \qquad (6b)$$

where the mass loss and the constants Λ and ζ now represent the sum of those processes which ablate material from the meteoroid in the form of atoms or molecules. Substituting this in equation (7a), we derive the luminosity equation:

$$I = \frac{\tau}{4} \frac{\Lambda A \delta_m^{-2/3}}{\zeta} m^{2/3} \rho v^5. \qquad (7b)$$

Öpik's semi-classical approach could, in theory, be improved upon by quantum mechanical methods. Few experimental data exist on collisional excitations by neutral atoms of this energy range (~100 e.v.). Consequently, Öpik's results are still in use, although we must consider this value as only a first approximation to the truth. He found the luminosity factor to vary as:

$$\tau = \tau_0 v \qquad (8)$$

where τ_0 = constant. Therefore

$$I = -\frac{\tau_0}{2} v^3 \frac{dm}{dt} = \frac{\tau_0 \Lambda A \delta_m^{-2/3}}{4\zeta} m^{2/3} \rho v^6. \qquad (9)$$

Thus, the physical problems become one of finding values for Γ, A, Λ, δ_m, ζ, and τ_0. The atmospheric density, ρ, has been obtained from recent rocket measurements (The Rocket Panel, 1952) and will not be considered as an unknown here.

B. The Meteor Data

To answer our questions we may call on theoretical, observational, and experimental techniques. We will review these tools briefly. We have already spoken of theoretical approaches to the problems of luminosity.

Observational data may be obtained photographically, visually, or by means of radar reflections from the ion column formed by the meteor. The last two sources will not concern us here. Let it suffice to state that the radar method can give us (1) the range of the meteor at the point of closest approach to the receiver, (2) the apparent angular velocity of the meteor at this point, (3) the line density of the ion column at this point and, under certain conditions, (4) the radiant or radiant distance of the measured point and from this, the space velocity of the meteor.

The value of visual observations was greatly reduced by the advent of the far more accurate photographic techniques. Furthermore, some statistical problems whose solution required the large number of visual observations are now best treated with the still more numerous and more accurate radar observations. And it is certainly not amiss to assume that statistical problems concerning the optical properties of meteors can be most accurately approached through reductions of large numbers of faint photographic meteors by the methods used in this work.

In the photographic program at Harvard, a pair of fast, wide angle cameras, 18 miles apart, are used to photograph the same meteor. The distance between the cameras is the baseline that supplies the distance scale. To provide a time scale, a shutter occults the optical system at known intervals, and intersperses the meteor trail with a series of breaks. Measures of these photographs yield directly the radiant and the height, velocity, and intensity as a function of time. In Chapter II we will describe an approximate method for finding these quantities. A summary of the more accurate method utilized by Whipple and Jacchia (in press) may be found elsewhere.

Photography of meteor spectra and time-lapse photographs of meteor trains have given additional information on the meteoric process. The reader interested in details may consult papers by Millman (1952, 1953) and by Cook and Millman (1955) for spectroscopic data, and papers by Whipple (1953) and by Liller and Whipple (1954) for the meteor train data.

Wind tunnel studies and measures of the flight and luminosity of high-speed pellets (Thomas and Whipple, 1951) (Rinehart, Allen and White, 1952) have yielded experimental results. Such work has given a good estimate of the drag coefficient, Γ, and set some limits on the coefficient of heat transfer, Λ.

We might also expect to include in the experimental data the results of studies of meteorites which yield values for the meteoric density, δ_m, the heat of vaporization, ζ, and, of course, chemical and physical composition in general. In that these data represent the only case where an astronomical result could be obtained directly in a terrestrial laboratory, they are unique. Unfortunately, however, they are misleading, for, as Whipple (1952) has shown for meteoric densities and as will be shown here for their physical structure, meteorites are not representative of meteors in general. Indeed, the difference between photographic meteors and meteorites could hardly be greater. It is difficult to find any other natural substance on the surface of the earth with the tenacity of an iron meteorite and, if our results are correct, material as fragile as the ordinary cometary meteoroid could not long exist under conditions on the earth's surface.

C. Some Important Earlier Work

Let us assume that the fundamental qualities that describe a meteor - the radiant and the velocity, height, and intensity as a function of time - have been measured, and let us apply the theory outlined in the first section to determine what we can about the meteor problems.

The mass of the meteoroid at any time is given by the integration of equation (9):

$$m(t) = \frac{2}{\tau_0} \int_t^{\infty} \frac{I}{v^3}\, dt, \qquad (10)$$

where $t = 0$ when the meteor is first detected. A lower limit of $t \longrightarrow -\infty$ is used to express the mass, before any ablation has taken place. Since the intensity of the meteor at the limit of detectability is usually very small compared to its maximum intensity, even a bad extrapolation of the light curve into the unobservable region will produce only a small error in the initial mass, $m(-\infty)$. (For convenience, this quantity is written as m_∞. A similar notation, V_∞, is used for the velocity of the meteor before it has suffered any deceleration.)

With the mass known, we may use equation (3) to determine the air density, ρ, to within the error imposed by our ignorance of the constants of that equation. Such data were among the first to give us information of the upper atmosphere (Whipple, 1939). Today, we can assume the density to be known from rocket measures and can invert the equation to obtain information about the meteor in terms of an observed constant, K_1:

$$K_1 = \Gamma A \delta_m^{-2/3} = -\rho^{-1} v^{-2} \left(\frac{2}{\tau_0} \int_t^{\infty} \frac{I}{v^3} dt \right)^{1/3} \left(\frac{dv}{dt} \right). \qquad (11)$$

Or, if we consider τ_0 to be an unknown as well, we get

$$K_1 \tau_0^{1/3} = -\rho^{-1} v^{-2} \left(2 \int_t^\infty \frac{I}{v^3} dt \right)^{1/2} \left(\frac{dv}{dt} \right) \qquad (12)$$

Whipple (1955) found that the observed values of this overall constant could not be satisfied by use of values of the individual constants thought to be reasonable. Specifically, if we accept the value of ΓA measured by Rinehart, Allen and White (1952) for high speed pellets, and the value of the luminous efficiency determined by Öpik, then the corresponding value of the meteoric density is about 0.3 gm/cm^3. If the luminous efficiency is increased to the maximum possible value (an efficiency of unity for the fastest meteors), the density is 1.7 gm/cm^3 - a value considerably less than that found for any meteorite. Such a value tempts us to speculate on the structure of a cometary meteoroid, but we will limit our discussion at this time to two remarks. First, Whipple has pointed out that these values are in qualitative agreement with his icy-conglomerate Comet Model (1950). Second, our knowledge of materials formed at near zero temperatures and pressures is admittedly small. One should guard against any preconceived ideas, based on his familiarity with terrestrial substances, when discussing the result cited above.

Another observationally determined constant, relating to the rate of mass loss, may be found. Dividing equation (6)

by equation (3), we obtain the relation

$$\frac{\Lambda}{2\Gamma\zeta} = \sigma = \frac{\dot{m}}{mv\dot{v}} = \frac{I}{\int_{-\infty}^{+\infty} \frac{I}{v^3} dt \; v^4 \dot{v}} \cdot \tag{13}$$

This may be integrated to give:

$$m = m_o \, e^{-\frac{\sigma}{2}(v_o^2 - v^2)} \, . \tag{14}$$

The measured values of σ, as determined by Jacchia, range from about 10^{-12} to greater than $10^{-10.5}$ $(\frac{sec^2}{cm^2})$. If we assume Rinehart's value of $\Gamma = 0.42$ and use the vaporization energy of stone or iron, say $5.6 \cdot 10^{10}$ ergs/gram, the observed values of σ determine a value of Λ (see Table 1).

Table 1

The Heat Transfer Coefficient Λ as Determined from Observed Values of σ.

$\sigma (sec/cm)^2$	Λ
10^{-12}	.047
$10^{-10.5}$	1.49

Not only is the range in values large, but the largest derived value exceeds the theoretical limit of unity for the fraction of their energy that the incoming air particles may transfer to the meteor. Furthermore, if we transfer all

energy, we transfer all momentum and our assumed value of Γ must be unity as well. This more than doubles the value of Λ in the extreme case and intensifies the discrepancy.

It might be suggested that the answer to the problem lies in the mode of ablation and indeed it probably does. Models of ablation, other than direct vaporization from the meteoroid, have been considered in order to explain the range and discrepancy in the observed values of σ. R. N. Thomas (1952) first showed that, on the basis of the classical heat transfer equation as applied to iron meteors, the heat conductivity toward the center would proceed too rapidly to allow the surface temperature to reach a value great enough to produce any appreciable amount of vaporization. He then considered the possibility that vaporization or melting and the shedding of droplets from a reaction zone at the surface was responsible for the loss of energy from the surface rather than the conduction of heat inward. He concluded that <u>if</u> droplets were dispersed from the surface, they would be small and the energy needed for this type of ablation would approach that required for vaporization. Thomas felt that only fragmentation, which can be nearly an energy-free process, could account for the scatter of the σ- values.

Although it is true that the meteoroid can lose material at the expenditure of less energy by melting or fragmentation, nevertheless the observations require that the material be in

the form of atomic particles at the time the luminosity is produced; i.e., if droplets do form, additional energy must still be supplied to vaporize the liquid, for we can observe only that mass which eventually reaches the vapor phase. The effect of the increased surface area due to the droplets or fragments will, however, affect the vaporization rate.

Following Jacchia's (1949) demonstration that meteor flares involved a loss of mass from the meteoroid, Henry J. Smith (1954) analyzed several bright meteors that displayed bright flares. He concluded that meteor flares were caused by the sudden fragmentation of a large number of small particles, of the order of 10^{-6} grams each.

Jacchia (1955) then made the significant contribution of the concept of the continuous fragmentation of meteors. His approach to the problems was primarily the empirical one needed to find some correction to the atmospheric densities derived from meteor decelerations.

Jacchia's early results, with bright meteors, agreed statistically with the values of atmospheric density obtained from rocket flights. For any one meteor which gave decelerations at more than one point, the density gradient found from the meteor data also agreed with the rocket data gradient. However, later results obtained from faint meteors photographed with the Super-Schmidt cameras showed distinctly anomalous decelerations. Although the decelerations near the beginning points of these meteors often gave a reasonable

value of the density, the meteors displayed too rapid a rate of deceleration, yielding density gradients that could not be reconciled with either the previous meteor or rocket results. We cannot improve upon Jacchia's own description of the solution of this discrepancy:

> "Fragments can be detached from the surface of larger meteor bodies without destroying their unity; but if fragments of similar size are detached from small bodies, this may mean their complete disruption into cluster of fragments. Larger meteors, then, will disintegrate only toward the end of their trajectories, while among fainter meteors the breakup may occur at earlier stages, even at the very beginning of the visible trail. What we obtain by integrating the brightness of a faint meteor is not the mass of a single body but a function of the total mass of all the fragments. The observed meteor deceleration, on the other hand, is the average deceleration of the brighter fragments and therefore larger than the deceleration of a single, unfragmented body."

In this brief review of some recent work, we have touched on two aspects of the meteor problem which we intend to amplify in this thesis. Whipple's discussion of the densities makes the assumption of fragile meteors reasonable, while the conclusions of Thomas and Jacchia on fragmentation almost necessitates the assumption. Our aim will be, in effect, to strengthen the concept of the fragile cometary meteoroid and to initiate a quantitative study of meteor fragmentation.

D. A Semi-Qualitative Approach to the Relationship Between Fragmentation and the Parameter σ.

Let us consider two special cases of meteoroids with a large surface-to-mass ratio. First, suppose the "meteoroid" to consist of a large number of small particles of the same size; each one interacts independently with the atmosphere but in the entire swarm the particles are sufficiently close together to allow our cameras to record them as a moving point source of light. We may think of this swarm as originating from a single body that has either fractured or melted and broken into droplets in the fashion of an over-sized rain drop. The mechanism is unimportant; the end result is an unlikely array which we wish to use to describe one extreme of subdivision. The question we wish to answer is: What value of σ would such a meteor yield? The observed deceleration would be that for an individual particle, since each particle reacts independently with the atmosphere. Let us set

$$A = \Sigma A_1 = NA_1, \tag{15}$$

$$m = \Sigma m_1 = Nm_1, \tag{16}$$

where A_1 and m_1 are the effective area and mass of the individual particle and N is their total number. The observed deceleration will be:

$$\dot{v} = - \frac{\Gamma A_1 \rho v^2}{m_1} . \qquad (17)$$

The amount of mass lost will be N times that lost by a single particle, or:

$$\Sigma \dot{m}_1 = \dot{m} = - \frac{\Lambda}{2\Gamma\zeta} N A_1 \rho v^3 . \qquad (18)$$

Dividing (18) by (17) we obtain

$$\frac{\dot{m}}{N m_1 v \dot{v}} = \frac{\Lambda}{2\Gamma\zeta} = \sigma . \qquad (19)$$

But $Nm_1 = m$ is just the value which we would obtain by integrating the intensity (equation 10) and would use in computing σ. We are left with the result:

$$\sigma = \frac{\dot{m}}{m v \dot{v}} , \qquad (20)$$

which represents no change from the case of a single body. From the observed value of σ, we could not detect the character of the meteor model proposed here. It should be clear, though, that such an object would be over-luminous, of short duration and would possess too great a deceleration.

As our second model, we assume the meteoroid to be essentially a source of particles only. In this instance we maintain a high area-to-mass ratio by a continuous fragmentation of particles but we do not greatly affect the deceleration. In the extreme case, the deceleration is a

function of the main meteoroid body and the mass loss is a function of a large number of smaller particles. The main body still suffers collisions with the air molecules - and is decelerated by them - but its surface area is too small, in comparison to the combined area of the particles, to produce an appreciable amount of vaporized material. The small particles, on the other hand, produce most of their light shortly after leaving the meteoroid, but they are continually replaced by new fragments. Denoting by A_p and m_p the total effective area and the mass of the fragmented particles, and by A_b and m_b the area and mass of the meteor body which is the source of these particles, we may write for the general case:

$$\dot{m}_p = - \frac{\Lambda}{2\zeta} A_p \rho v^3, \tag{21}$$

$$\dot{m}_b = - \frac{\Lambda}{2\zeta} A_b \rho v^3, \tag{22}$$

where $\dot{m}_b$ represents the mass lost by the meteoroid by <u>direct</u> vaporization. Then, the total mass per second introduced into the atmosphere in the form of vaporized material is:

$$\dot{m}_p + \dot{m}_b = \dot{m} = - \frac{\Lambda}{2\zeta} \rho v^3 \, (A_p + A_b). \tag{23}$$

The observed deceleration will be:

$$\dot{v}_b = - \frac{\Gamma A_b \rho v^2}{m_b}. \tag{24}$$

Dividing (23) by (24), we obtain

$$\sigma_{obs} = \frac{\dot{m}}{m_b v \hat{v}_b} = \frac{\Lambda}{2\Gamma\zeta}\left(1 + \frac{A_p}{A_b}\right) = \sigma\left(1 + \frac{A_p}{A_b}\right). \qquad (25)$$

Consequently, when we compute the quantity on the left side of equation (25), we do not obtain a number which is solely a function of those physical constants that describe the behavior of meteors in the atmosphere. Instead, we determine some number which will be larger (unless $A_p = 0$) than $\sigma = \frac{\Lambda}{2\Gamma\zeta}$.

We must mention also another complicating factor which will alter equation (25). We must question our observed value of m_b. There will always be a certain number of fragments which have left the major body but have not yet vaporized. These particles will not be observed as "mass lost" until some later instant when the vaporization has occurred. Consequently, we will always be overestimating the mass, m_b, of the parent body by the amount of mass contained in these fragments. Similarly, we will be overestimating the area, A_b, of the parent body. The deceleration, $\hat{v}_b$, is a directly measured quantity and is related to the actual mass of the parent body, not to the mass we derive by integrating the light curve. Therefore, we have, in effect, divided apples by bananas in equation (24). The same is true for the factor A_b in equations (22) and (23). Here we should have used a smaller area to determine the mass loss by direct vaporization from the parent body. To adjust these quantities to their correct values, let us set:

$$k\, m_b = m_b' \text{ where } k < 1, \tag{26}$$

and

$$k_A\, A_b = A_b' \text{ where } k_A < 1, \tag{27}$$

and where the primes indicate the correct values. If we assume that the parent body has the same shape (see equation 2) before and after it has fragmented the particles, we can write

$$k_A = (k)^{2/3} \tag{28}$$

and equation (27) becomes:

$$(k)^{2/3} A_b = A_b'. \tag{29}$$

We may now rewrite equation (25) in its proper form as:

$$\frac{\dot{m}}{k m_b v \dot{v}_b} = \sigma \left(1 + \frac{A_p}{(k)^{2/3} A_b}\right) = \sigma'_{obs}, \tag{30}$$

or, multiplying equation (30) by k,

$$\sigma_{obs} = \sigma \left(1 + \frac{A_p}{(k)^{2/3} A_b}\right) k = k\, \sigma'_{obs}. \tag{31}$$

For a numerical example, we may rewrite this equation for the special case where: (1) all fragments and the parent body are spherical and have the same density; and (2) all fragments are of the same mass, m_1. Then the total mass of the particles is:

$$m_b\ (1 - k) = \Sigma m_i = N\ m_i, \qquad (32)$$

where N is the number of such particles.

The radius of each particle will be:

$$r_i = \left(\frac{m_i}{4/3\pi\delta_m}\right)^{1/3} = \left(\frac{3m_b(1-k)}{4\pi\delta_m\ N}\right)^{1/3}. \qquad (33)$$

The effective area of all particles is then:

$$A_p = N\pi \left(\frac{3m_b(1-k)}{4\pi\delta_m\ N}\right)^{2/3}. \qquad (34)$$

Similarly, the effective area of the parent body is:

$$A_b' = \pi\left(\frac{3m_b\ k}{4\pi\delta_m}\right)^{2/3}. \qquad (35)$$

Substituting these results in equation (31), we find that

$$\sigma_{obs} = \sigma\left[1 + (Nk)^{1/3}\ (1-k)^{2/3}\right]. \qquad (36)$$

To obtain an idea of the degree of fragmentation needed to explain some of the observed discrepancies of σ we have computed some combinations of k and N which give a value of $\frac{\sigma_{obs}}{\sigma} = 10$. Table 2 gives these results (computations made for 0.1 gram meteor).

Table 2

Values of k and N Necessary to Give $\frac{\sigma_{obs}}{\sigma} = 10$ for 0.1 gram meteor (See Text)

k	N	m_1 (grams)
0.90	$8.1\ 10^4$	$1.2\ 10^{-7}$
0.75	$1.6\ 10^4$	$1.6\ 10^{-6}$
0.50	$5.8\ 10^3$	$8.6\ 10^{-5}$
0.25	$5.2\ 10^3$	$1.4\ 10^{-5}$
0.10	$9.0\ 10^3$	$1.0\ 10^{-5}$

We should point out that this approach is not limited to the case discussed above. The reader will see that it may be easily generalized for any distribution of particle sizes. There may be, for example, a number of parent bodies, each of which is fragmenting. In this case, the deceleration would apply to the largest of these. Also, the solution may be generalized to include shapes other than spherical or to include separate densities for the fragments and the parent bodies. But as we shall see in Chapter IV, such refinements can be of academic interest only -- the observations will not be sufficiently good to determine so many separate variables.

CHAPTER II

NEW DATA AND THE METHOD OF APPROXIMATE REDUCTIONS

A. The Super-Schmidt Meteor Cameras

The data for this thesis are derived almost entirely from double-station photographs obtained with the four Baker Super-Schmidt meteor cameras operated by the Harvard Meteor Project at Soledad Canyon and Dona Ana Stations in New Mexico and supported by contracts with the U. S. Naval Bureau of Ordnance, the Office of Naval Research and the U. S. Air Force. These instruments and their auxiliary equipment are described in some detail elsewhere (Whipple, 1951), (Carrol, McCrosky, Wells and Whipple, 1951). A schematic diagram of the optical system (Figure 1) and an enumeration here of some pertinent quantities will be sufficient to explain the reduction technique.

Table 3

Physical and Optical Properties of the

Baker Super-Schmidt Meteor Cameras

Aperture	12.25 inches
Effective Focal Length	7.94 inches
Effective Focal Ratio	0.82
Field	55°
Focal Surface	spherical section of radius 7.9 inches, chordal diameter 7.4 inches
Shutter Speed	1800 r.p.m.

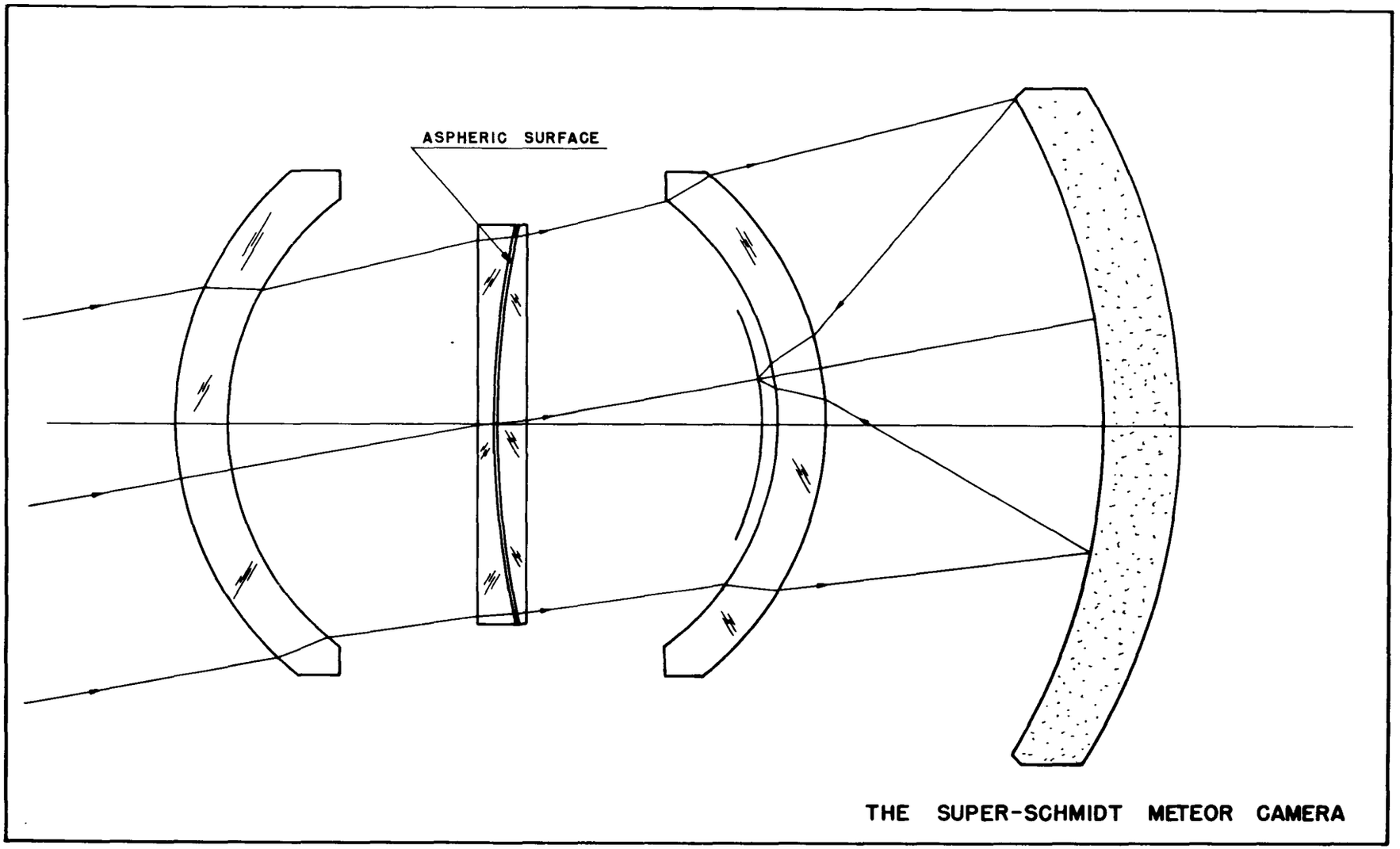

THE SUPER-SCHMIDT METEOR CAMERA

The rotating shutter lies about one-quarter of an inch outside of the focal surface. It is a spherical section concentric with the focal surface. The size and location of the shutter openings are shown in Figure 2.

The image quality is uniform over the field. Coma is detectable in brighter images but at least 50 percent of the intensity of a point source falls on a circle of 15 μ diameter. There is essentially no distortion of the spherical projection of the sky.

All photographs of meteor trails have been obtained on Eastman-Kodak X-Ray film. The film is molded, under heat and pressure, to the shape of the focal surface (Carrol et al., 1951). Although the film has not been shown to receive a permanent set to the spherical section, measures of one-year old film show little or no deviation from the original curvature. The general characteristics of the X-Ray film are similar to those of the Eastman I-O Spectroscopic emulsion. That is, it is a fast, blue sensitive emulsion with considerable graininess. Its high reciprocity failure is ideal for meteor photography, since it minimizes the density due to star and night sky light. Sky fog becomes serious with an effective exposure of more than three minutes. Since the rotating shutter excludes three-quarters of the light, exposures of 12 minutes duration are feasible with this emulsion.

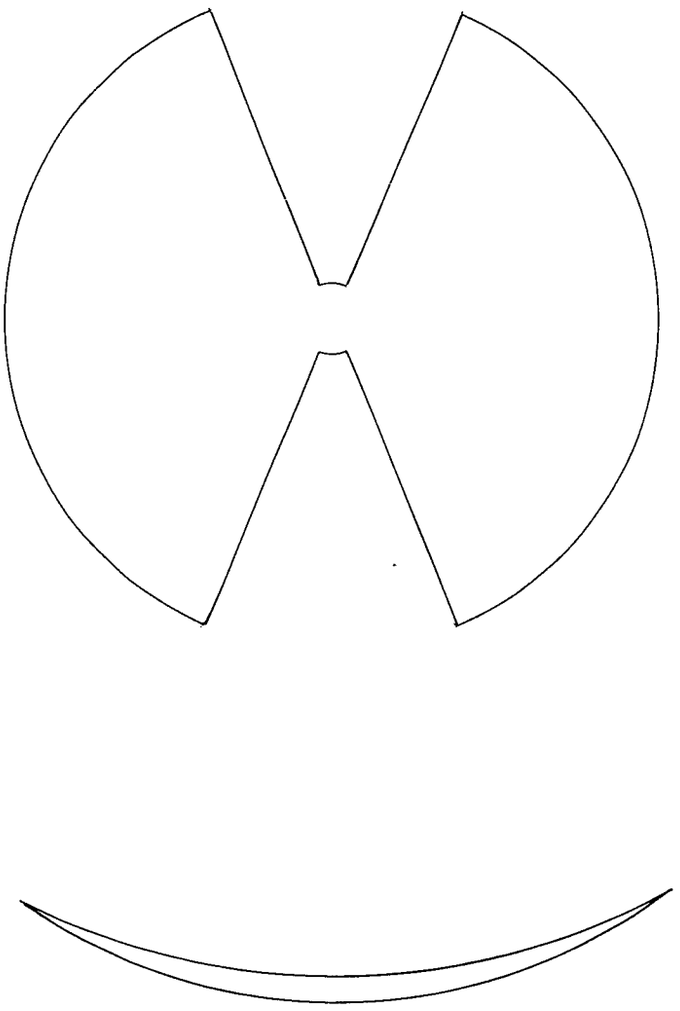

FIGURE 2

PLAN VIEW AND RADIAL SECTION
OF METEOR CAMERA SHUTTER

The exceptional effectiveness of the camera and emulsion are best described in terms of actual performance. Meteors are photographed at a rate of about one per 18 minutes of exposure. The visual magnitude of the faintest meteor images is of the same order as the limiting magnitude seen by the naked eye.

B. Meteor Heights

When the approximate reduction program was first considered, the criteria for a "satisfactory" method were rather vague. However, from the experience gained in the accurate reduction program, one could be certain that data with errors as small as 1 percent in velocities and heights could not be obtained with a reasonable expenditure of time. At the other extreme, one could question the value of statistics derived from data with mean errors of about 10 to 15 percent. With these limitations on the accuracy, a search for a sufficiently rapid method was made. To anticipate the general result of this attempt, we may state that the method to be described yields mean errors of about 5 percent. Thirty minutes is required to complete the reduction of a meteor pair. The method can be best explained if we first derive the necessary equations, next discuss separately the methods of measurements, and finally, return to the equations and estimate the magnitude of errors due to various simplifying assumptions and to errors of measurement.

The geometry of the problem can be seen in Figure 3, where R_{AB} is the distance between stations; R_A is the distance from Station A to some point on the meteor path, R_B is the distance from Station B to the same point in space. This point, on either meteor trail, will be referred to as a common point (C). The orientation in space of the triangle (A, B, C) is described by the declination (δ) and the hour angle (t) coordinates. (See Figure 3). R_{AB}, δ_{AB} and t_{AB} are constants of the stations. The hour angle and declination represent the direction of the Dona Ana Station as seen from the Soledad Station. The stations were surveyed by the White Sands Proving Grounds. Their results and the station constants are given in Table 4.

Table 4

Constants for New Mexico Stations

	Soledad Canyon	Dona Ana
Altitude (km)	1.57	1.41
Latitude	32° 18' 06"	32° 30' 22"
Longitude	106° 36' 38"	106° 47' 58"
R_{AB}	28.80 km	
t_{AB}	+124°.7	
δ_{AB}	+ 41°.5	

From the spherical triangle, (Pole, P_{AB}, P_1), we solve for γ_1, the angle between the direction to the meteor and the

direction of the line joining the stations:

$$\cos \gamma_i = \sin \delta_i \sin \delta_{AB} + \cos \delta_i \cos \delta_{AB} \cos(t_{AB}-t_i). \quad (37)$$

The subscript i refers to either Station A or Station B. With γ_A and γ_B determined, the values of the ranges, R_A and R_B are found from:

$$R_i = R_{AB} \frac{\sin \gamma_j}{\sin(\gamma_B-\gamma_A)}, \quad i \neq j. \quad (38)$$

The height of the common point above ground, assuming a flat earth, is then:

$$h_i = R_i \cos Z_i, \quad (39)$$

where Z is the zenith distance of the common point and cos Z is given by the equation:

$$\cos Z_i = \sin \phi \sin \delta_i + \cos \phi \cos \delta_i \cos t_i. \quad (40)$$

We have used for the latitude, ϕ, the average value of the two stations.

Clearly the same point in space can be described by only one height, and thus $h_A \equiv h_B$. This comparison gives the first check on the computations.

The height above sea level, H, is found by assuming h to be measured from an elevation equal to the mean elevation of the two stations. In kilometers:

$$H = h + \Delta h$$
$$= h + 1.5. \quad (41)$$

Solutions for equations (37) and (38) were prepared in graphic form in order to eliminate the tedious and time-consuming task of directly forming such solutions many thousands of times.

Since both γ and cos Z are functions of δ_1 and t_1, a solution for cos Z was also prepared and superimposed on the chart for γ. These charts will not be reproduced here. They are applicable only to the data acquired at the Soledad Canyon and Dona Ana Stations, and therefore are not of great interest. Table 5 summarizes the information obtained from these graphs and from another to be discussed later.

Table 5

Description of Graphs Utilized in the Approximate Reductions

Graph	Enter with	Read	Accuracy
Ia	$-10° \leq \delta_1 \leq 90°$ $-50° \leq t_1 \leq 50°$	γ_1	0°.1
Ib	Same	cos Z	0.01
II	$60° \leq \gamma_1 \leq 135°$ $60° \leq \gamma_2 \leq 135°$	R_1	1 km
III	Same	R_2	1 km
IV	$.50 \leq A \leq 1.00$ $0° \leq B \leq 20°$	sin r	.001

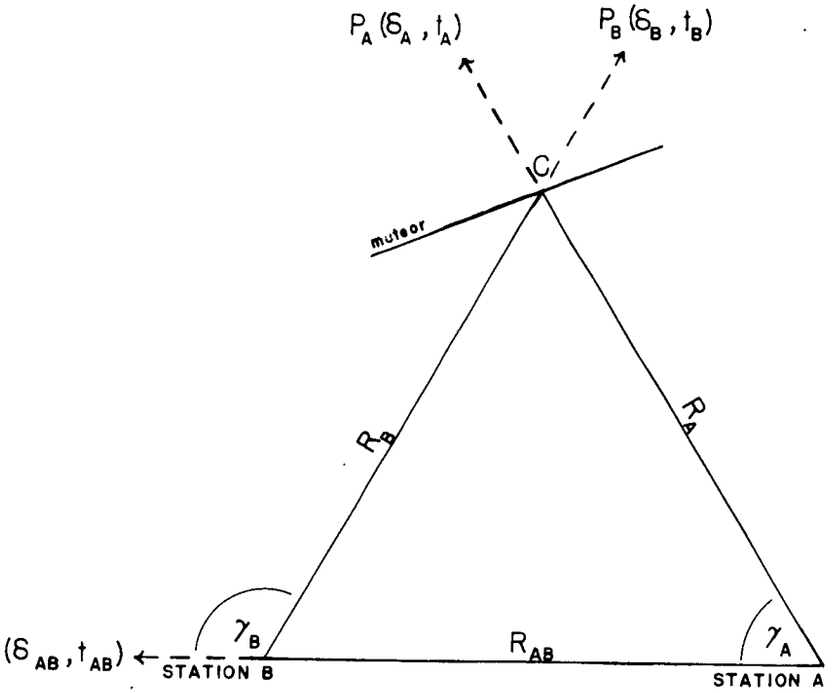

FIGURE 3
RELATIONSHIP OF GEOMETRICAL QUANTITIES
USED TO DETERMINE METEOR HEIGHTS

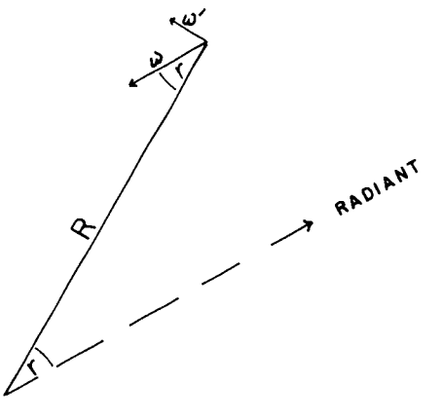

FIGURE 4
RELATIONSHIP OF GEOMETRICAL QUANTITIES
USED TO DETERMINE METEOR VELOCITIES

C. Velocities and Radiants

The meteor trail is interrupted every 1/60 sec by one of the occulting sections of the rotating shutter. These breaks in the trail allow one to measure the apparent angular velocity of the meteor at some point along its trajectory. This measure is referred to as the apparent angular velocity since only the component normal to the line of sight is measured. In general, such measures are made on both photographs of the meteor at the position of the common points.

Figure 4 shows the relationships between the apparent angular velocity, ω'; the angular velocity, ω; and the radiant. From this diagram we see that:

$$\omega_i = \frac{\omega'_i}{\sin r_i} , \qquad (42)$$

where r_i is the angular distance from the radiant to the common point. The space velocity, v, is then given by the equation

$$v_i = \frac{\omega'_i R_i}{\sin r_i} , \qquad (43)$$

where R_i is the range found in the solution for heights. As in the case of the heights, the velocities obtained from the two photographs should agree.

For computing purposes, equation (43) is written as:

$$v_i = \frac{.314\, R_i}{\sin r_i} \left(\frac{\text{Distance}}{\text{Break}}\right), \qquad (44)$$

where the quantity $\left(\frac{\text{Distance}}{\text{Break}}\right)$ is the distance between dashes on the film in units of 1/24", the units of the measuring engine we employed.

For equation (44) to be applicable, we must have determined the position of the radiant. When the two meteor trails intersect at a small angle, Q, it is difficult to find an accurate radiant point. In such cases another approach to determine the velocity is desirable. From equation (43) we have:

$$v_A = v_B = \frac{\omega_A' R_A}{\sin r_A} = \frac{\omega_B' R_B}{\sin r_B}, \qquad (45)$$

or

$$\frac{\sin r_A}{\sin r_B} = \frac{\omega_A' R_A}{\omega_B' R_B} \equiv A, \text{ by definition.} \qquad (46)$$

If the apparent angular velocity is measurable on both trails of a meteor pair, A may be computed. This gives one relationship between r_A and r_B. For meteors with a small Q, it is possible to measure $r_A - r_B$ (or $r_A + r_B$) with good accuracy. That this is true can be most easily seen by considering the extreme case of a meteor pair intersecting at $Q = 0°$ (or $Q = 180°$); i.e., both trails lie on the same great circle. Then the distance between the two common points will be exactly:

$$r_A - r_B = B \text{ (or } r_A + r_B = B\text{), by definition.} \qquad (47)$$

The simultaneous equations (46) and (47) may be solved for sin r_A and sin r_B. This solution was prepared in graphic form (see Table 5, Graph IV). With these values of r_1, v is found from (44). We have called velocities determined in such a fashion "indirect velocities" as distinct from the velocities obtained from meteors where a direct measure of the radiant is possible (direct velocities). It will be noted from equation (45) that we have forced the indirect velocities determined from each trail to agree. This comparison offers a check on the computations.

The position of the radiant may be obtained by finding the intersection of two small circles of radii of r_A and r_B with centers at P_A and P_B, respectively. In general such circles will intersect twice, but a quick inspection of the trails is sufficient to distinguish the spurious radiant point.

D. The Reduction Procedure

In this section we shall carry through the complete reduction of an imaginary meteor pair. Our purpose is not primarily one of instruction in technique, but to present, in logical sequence, the various difficulties and approximations that are present so that the reader may acquire a realization of the limitations of the method.

A separate computing form is used for each meteor. Table 6 is such a form. Certain data necessary for each meteor are copied from the card catalogue maintained for all Harvard Meteors. These include:

a) meteor serial number for each trail.

b) camera designation (SS, ST, SK, SL) and plate number for each film.

c) region of the plate center, given by δ and α.

d) astronomical date of the exposure.

e) time of meteor occurrence, to .01 minute if the meteor was observed visually; or the mean time of the exposure if no visual observation was available.

The local sidereal time, in degrees, of the nearest midnight ($L\theta_o$) is obtained for the date. To this is added a correction to obtain the local sidereal time ($L\theta_i$) of the meteor instant.

The preceding section makes it clear that the entire method depends heavily on our ability to locate on each film a point on the meteor trails that represents the same point in space, the common point. If the meteor shows a burst or some other discontinuity in the light curve, a common point is obvious. However, the faint meteors, with which we are primarily concerned here, usually have smooth light curves. In these cases a more subtle technique is necessary. The

	BY:	DATE:
Records	....	....
Com'n p'nt	....	....
Plotter	....	....
Computer	....	....

Meteor		—		—	
Plate	S	—	S	—	
Region					
α, δ					
Date, $L\theta_o$			—	—	
MST, $L\theta_1$				—	
Star Pos.					
No.					
t					
δ					
Direction		—		—	
Magnitude					
Com'n p'nt	n_1		n_2		
	SC	DA	SC	DA	
Quality					
n					
δ					
t					
cos Z					
γ					
h					
H					
R					
Projec't					
Dis't/Brk	/	/	/	/	
$r_{SC}-r_{DA}$ ~~$V_{SC}-V_{DA}$~~					
A					
sin r					
Velocity					
Radiant					
Q					
t, δ, α					
Shower					
cos Z_{rad}					
Wake					
Start: n, H					
End: n, H					
					Accurate reduction data in red.

Table 6

Computing Form for Approximate Reduction Method

number of dashes visible on each trail is counted and, if it is the same, we assume that dashes with the same ordinal number are common points.

Such an assumption fails in three minor respects. Firstly, the shutters are not synchronized, i.e., we do not know the orientation of one shutter with respect to the other at any given instant. Consequently the common point can be in error by as much as half the distance between dashes. Secondly, the focal plane shutter interrupts the same position of the film at constant time intervals. The rate at which the meteor is interrupted depends on its direction of motion and its apparent velocity on the film. In the extreme case of a meteor trail passing through the film center, an error of one dash can be made. But since the two trails of a meteor pair are usually similar in their direction of travel on the film, and since their apparent velocities on the film are small compared to the shutter velocity, the error will generally be only a small fraction of a dash. Thirdly, in assuming that breaks with the same ordinal number are common points, we assume that both cameras have photographed the meteor to the same limiting absolute magnitude or, alternatively, that the differential distance correction from the beginning to the end of the meteor is small or the same for both trails. Since most of our trails are short, the differential distance correction is small.

We can conclude that the common points chosen on trails showing the same number of breaks will be accurate to within one dash. However, the two cameras often do not record the same number of breaks for the following reasons:

a) The sensitivities of the cameras are not equal. With increasing experience in figuring the correcting plate, the manufacturer has been able to improve the quality of each succeeding camera. The effect is most noticeable when comparing trails obtained on the first (SS) and second (ST) Super-Schmidts.

b) The apparent magnitude of the meteor as seen from the two stations may differ by several tenths of a magnitude because of distance corrections. Effects (a) and (b) often compensate one another in part since the earlier camera, at Soledad Station, is directed more nearly toward the zenith than is the mate camera at the Dona Ana Station.

c) The effective exposure time per dash is proportional to ω_i'. Thus, the trail nearer the radiant is photographed as a brighter image and the plate limit is reached at a fainter absolute magnitude.

Effects (a) and (b) combined are usually minor compared to effect (c). By noting the general shape of the meteor light curve of the brighter trail, one can obtain an acceptable common point by estimating the number of dashes that failed to be recorded at the beginning and at the end of the fainter meteor trail. In only a very few cases did the combination of the factors of effective sensitivity of the camera, and the apparent velocity of the meteor, differ so much that no acceptable common point could be found. For each common point, we record under "Quality" (Table 6), an estimate of the number of dashes by which the common point may be in error. This never exceeds 3 for an acceptable meteor and rarely exceeds 2.

To mark the common points, a small piece of Scotch Tape is placed on the reverse side of the film at the location of the trail. Ink dots placed on this tape indicate the common point. For longer meteors (20 dashes or more), two common points, (n_1 and n_2 in Table 6) are chosen in order to make a check on the entire reduction. The common point is recorded as the ordinal number of the dash, the dash nearest the radiant being called "1". The duration of the meteor is measured in terms of the total number of visible dashes, N. The beginning of the trail is specified by noting, under "Direction", the octant, as seen from the meteor, in which the radiant lies.

To measure the celestial coordinates of the common points and radiant, we utilize a transparent Plexiglass hemisphere of 8-inch radius, calibrated in hour angle and declination. The scale of these calibrations and the radius of the globe correspond to the scale and radius of the Super-Schmidt films. To read the coordinates of the common point, we need only to position the film properly on the globe. We accomplish this by choosing three or four bright stars which appear on one of the films, determining the declination and hour angle of these stars at the time of the meteor, and plotting these star positions on the globe. The film is then placed on the globe so that the star images and their plotted positions coincide. Since the regions of the two mate films overlap in an area of approximately one-quarter of the film, we can position the second film by superimposing stars in this region. The hour angle and declination of the common points are then read from the globe scales.

We determine the radiant and radiant distances, r_A and r_B, with the aid of a pair of curved rulers of 8-inch radius and 90° length, attached to one another by a hinge. They are calibrated in degrees, the pivot point of the hinge being zero degrees. When each rule lies parallel to one of the meteor trails, the zero point represents the radiant. The radiant distances are read from the rules and the coordinates of the radiant point are read from the hemisphere. The

cosine of the zenith distance of the radiant ($\cos Z_R$) is determined from Nomogram Ib.

The quantity Q is the angle of intersection of the two trails. An estimate of this quantity, accurate to about 10 percent, is made when the radiant is found. The value of this angle is not used in the reductions but it serves as a measure of quality of the directly determined radiant.

The apparent angular velocity, or distance per break, is measured on the Harvard Coast and Geodetic measuring machine. This has been equipped with a section of an 8-inch radius Plexiglass sphere for the support of the film. The spherical section is large enough to permit all measurements to be made with the optical axis perpendicular to the image when the trail occurs at the edge of the film. This reduces the focussing problem and also allows us to neglect any correction for the projection effect which would be necessary if the curved film rested on the flat carriage of the measuring engine.

The number of breaks measured depends on the apparent angular velocity of the trail. In general, we attempt to measure a distance of from 1 to 3 mm, which may represent 2 to 8 breaks. The measurements are usually made from the end of one dash to the end of another; that is, an integral number of dashes is measured. Corrections, by eye, are made for the photographic spreading of the image if the two terminal dashes of the measured trail section do not appear to be of about the same intensity. The dashes to be

measured are chosen in such a way that the common point lies in the center of the measured section.

The trails are inspected for any wake, terminal blending or marked abnormalities in the distribution of light over the trail. The position and apparent magnitude of the brightest dash may be measured. The method of meteor photometry has been described by Jacchia (1949). The photometry has been completed on only a limited number of the meteors dealt with here.

This completes the measurements made on a meteor pair. We then determine, from the equations given earlier, cos Z_1, γ_1, R_1, h_1, H, A and v_1, in that order.

To complete this outline of the method, we will add a description of an earlier approach to the problem of finding common points. The argument, due to Olivier (1925), proceeds as follows: Consider the plane defined by the two stations and a point on the meteor. The lines R_A, R_B and R_{AB} lie in this plane which intersects the celestial sphere on a great circle. Then the position of the meteor point as seen from each station must lie on a great circle which also includes the celestial position of one station as seen from the other. Conversely, if the two meteors are located properly on the globe, we can draw a great circle through the point defining the direction between the stations. Then, by the argument above, the intersections of this great circle with the meteor trails must represent

common points. This technique was tried and discarded as being too insensitive for most cases. In practice, we employed a movable great circle which was attached to the measuring globe and pivoted at the points (δ_{AB}, t_{AB}) and ($-\delta_{AB}$, t_{AB} -180°). When the meteor trails formed a moderately small angle with this circle, the common points could be varied by several dashes with only a slight shift of the films. If the time of the meteor occurrence is lacking, the precise position of the film on the celestial sphere is unknown.

E. Single-Station Shower Meteors and the Approximate Method

The program of meteor astronomy at the Harvard College Observatory, includes the investigation of the origin and histories of the shower meteors by study of the distribution of the radiants over the period of the shower (see, for example, Wright, Jacchia and Whipple, in press). Single-station meteors are used in a least-squares solution to determine the radiant, if they appear to belong to the shower; that is, if an extension of the trail passes through (or near) the assumed radiant point for the time of the meteor, and if visual inspection determines that the apparent angular velocity of the meteor is reasonable for the shower velocity and the radiant distance. A small amount of work with the globe used in the approximate method removes

the guesswork from this visual determination. By assuming that the meteor belongs to the shower, we can estimate a height that corresponds to that of meteors of the shower velocity. The apparent angular velocity (ω_1'), cos Z_1, and the distance from the assumed radiant (r_1), are measured for some point on the trail. From equations (39) and (43), we have:

$$v = \frac{\omega_1' h_1}{\cos Z_1 \sin r_1} . \qquad (48)$$

If the meteor belongs to the shower, the measured values should yield the shower velocity. We may be deceived occasionally by meteors whose true radiants and velocities are not those of the shower but combine, by chance, in such a way that

$$(v \sin r_1)_{\text{shower}} = (v \sin r_1)_{\text{non-shower}} .$$

Such cases must be far more rare than the 10 percent of single-station meteors which we have been able to eliminate from those meteors thought to belong to the shower.

It is probably obvious that the usual approximate method may also be used to eliminate those double-station meteors that have the proper radiant but a non-shower velocity.

F. Height Errors

The problem of errors in our data reduction includes two major questions, neither of which has yet been finally answered. First, the velocities and radiants determined by

the direct and indirect methods are, in general, at variance with one another. We need some quantitative criteria for making a choice between the two results. Second, we desire a more exact knowledge of the mean errors as a function of the various parameters of the solution. That neither of these desiderata have been found does not affect the results of this thesis to any reasonable extent. All the problems treated here are of such a nature that we need not be concerned with whether the errors are 3 percent or twice that amount. However, we will wish to know that the errors are not, say, 15 percent. Our brief study of errors will show they are not.

The final answers to these questions will be found only after the completion of the reduction project. Eventually we intend to acquire approximate data on 2000 meteors, including about 300 faint meteors that have been reduced by a more accurate method. An intercomparison of results should supply the information we want. Comparison can now be made with several hundred brighter meteors already reduced by Jacchia. However, the accuracy we would obtain in determining the radiant of these long meteors will seldom be approached for fainter meteors. On the other hand, common points are often more difficult to obtain on long meteors. All in all, we do not consider bright meteors to be comparable to faint ones with regard to our system of

measuring. A comparison of velocities obtained by accurate methods and by the present method has been made for some 25 bright meteors. Our average error in velocity was about 3 percent.

With respect to the order-of-magnitude estimate we can study the results of measuring errors of probable amounts and we may compare our results for shower meteors with their known values.

Let us begin with the errors in height introduced by our assumption that the earth is a plane surface. The correction for this was ignored as being small compared with the intrinsic errors of measurement. This is true if the meteors are in the vicinity of the zenith, as they were in all the early New Mexico photographs treated here. It is easily shown that

$$\Delta h = h - h' = \frac{R^2 - h'^2}{D}, \tag{49}$$

where h is the computed height above the station level, h' is the true height above the station level, R is the range from meteor to station, and D is earth's diameter. With the assumption that

$$\Delta h \ll 2h, \tag{50}$$

we obtain

$$\Delta h \doteq \frac{R^2 - h^2}{D + 2h}. \tag{51}$$

Employing equation (39), we may write

$$\Delta h \doteq \frac{h^2(\sec^2 Z - 1)}{D + 2h}. \qquad (52)$$

For meteors of 100 km altitude, the correction factor reaches 0.5 kilometers at a zenith distance of 37°.7. Essentially none of the meteors in this work exceed this value. The average zenith distance is of the order of 20°.

If the common point is improperly chosen or measured, or if the two films are not correctly positioned on the globe, the two range lines, as defined by (δ_A, t_A) and (δ_B, t_B) will either not intersect in space or will not intersect on a point on the meteor trail. Whether the intersection occurs for any given set of measures or not, our computations still lead to a complete description of some triangle which represents, to some degree of approximation, the true triangle defined by the two stations and a point on the meteor. We are interested in knowing how good an approximation our measures probably give. To investigate this, it will be most convenient to study, in the original equations, the changes brought about by independent changes in the assumed position of the common point along the t and δ axes. Differentials of equations (37), and (40), (38) and (39) yield:

$$\left(\frac{\Delta\gamma}{\Delta\delta}\right)_t = - \frac{\cos\delta \sin\delta_{AB} + \sin\delta \cos\delta_{AB} \cos(t_{AB}-t)}{\sin\gamma}, \quad (53a)$$

$$\left(\frac{\Delta\gamma}{\Delta t'}\right)_\delta = - \frac{\cos\delta_{AB} \sin(t_{AB}-t)}{\sin\gamma}, \quad (53b)$$

$$\left(\frac{\Delta Z}{\Delta\delta}\right)_t = - \frac{\sin\phi \cos\delta + \cos\phi \sin\delta \cos t}{\sin Z}, \quad (54a)$$

$$\left(\frac{\Delta Z}{\Delta t'}\right)_\delta = \frac{\cos\phi \sin t}{\sin Z}, \quad (54b)$$

$$\left(\frac{\Delta R_A}{\Delta\gamma_A}\right)_{\gamma_B} = \frac{R_{AB}}{57.3}\left\{\frac{\sin\gamma_B \cos(\gamma_B-\gamma_A)}{\sin^2(\gamma_B-\gamma_A)}\right\}, \quad (55a)$$

$$\left(\frac{\Delta R_B}{\Delta\gamma_B}\right)_{\gamma_A} = - \frac{R_{AB}}{57.3}\left\{\frac{\sin\gamma_A \cos(\gamma_B-\gamma_A)}{\sin^2(\gamma_B-\gamma_A)}\right\}, \quad (55b)$$

$$\left(\frac{\Delta R_A}{\Delta\gamma_B}\right)_{\gamma_A} = - \frac{R_{AB}}{57.3}\left\{\frac{\sin\gamma_A}{\sin^2(\gamma_B-\gamma_A)}\right\}, \quad (55c)$$

$$\left(\frac{\Delta R_B}{\Delta\gamma_A}\right)_{\gamma_B} = \frac{R_{AB}}{57.3}\left\{\frac{\sin(\gamma_B)}{\sin^2(\gamma_B-\gamma_A)}\right\}, \quad (55d)$$

$$\left(\frac{\Delta h}{\Delta\delta}\right)_t = \cos Z \left(\frac{\Delta R}{\Delta\delta}\right)_t - \frac{R}{57.3}\left[\sin Z \left(\frac{\Delta Z}{\Delta\delta}\right)_t\right], \quad (56a)$$

$$\left(\frac{\Delta h_i}{\Delta\delta_j}\right)_{t_j} = \cos Z_i \left(\frac{\Delta R_i}{\Delta\delta_j}\right)_{t_j}, \; i \neq j, \quad (56b)$$

$$\left(\frac{\Delta h}{\Delta t'}\right)_\delta = \cos Z \left(\frac{\Delta R}{\Delta t'}\right)_\delta - \frac{R}{57.3}\left[\sin Z \left(\frac{\Delta Z}{\Delta t'}\right)_\delta\right] \text{ and} \quad (56c)$$

$$\left(\frac{\Delta h_i}{\Delta t'_j}\right)_{\delta_j} = \cos Z \left(\frac{\Delta R_i}{\Delta t'_j}\right)_{\delta_j}, \quad i \neq j. \tag{56d}$$

The subscripts on the differentials refer to those variables held constant during the differentiation. The differential angles are all expressed in degrees of arc, having been converted from radian and from degrees of hour angle when necessary. The parameter

$$\Delta t' = \Delta t \cos \delta. \tag{57}$$

We will discuss the errors involved in one particular case. Computations for other cases show that the total errors will be similar in other parts of the sky where meteors have been photographed. As our example, we will use a meteor with the common point coordinates given in Table 7. The remaining values in the table were computed from the equations previously given. The accuracy, of course, exceeds that which may be obtained from reading the nomograms and also exceeds the amount commensurate with the ultimate accuracy of the measures (0°.1).

It is a bit difficult to estimate a reasonable amount for the errors in the common point, positioning, or measuring which combine to give the total errors, $\Delta\delta$ and Δt.

Table 7

Differential Errors Produced by an Error in the Common Points

		Station A	Station B
δ		+27.6	+13.9
t		+13.5	-0.4
γ		86.2	105.0
R	(km)	86.31	89.16
cos Z		.976	.948
h	(km)	84.2	84.5
H	"	85.8	85.9
$\left(\frac{\Delta R_1}{\Delta \gamma_1}\right)_{\gamma_j}$	$\frac{\text{km}}{\text{degree}}$	+4.43	-4.57
$\left(\frac{\Delta R_1}{m\gamma_j}\right)_{\gamma_1}$	"	-4.83	+4.68
$\left(\frac{\Delta \gamma}{\Delta \delta}\right)_t$	$\frac{\text{degree}}{\text{degree}}$	-0.714	-0.773
$\left(\frac{\Delta Z}{\Delta \delta}\right)_t$	"	-0.433	-1.000
$\left(\frac{\Delta R_1}{\Delta \delta_1}\right)_{t_1}$	$\frac{\text{km}}{\text{degree}}$	-3.16	+3.53
$\left(\frac{\Delta R_1}{\Delta \delta_j}\right)_{t_j}$	"	+3.73	-3.34
$\left(\frac{\Delta h_1}{\Delta \delta_1}\right)_{t_1}$	"	-2.94	+3.84
$\left(\frac{\Delta h_1}{\Delta \delta_j}\right)_{t_j}$	"	+3.64	-3.17

Table 7 (continued)

		Station A	Station B
$\left(\frac{\Delta Y_i}{\Delta t'_i}\right)_{\delta_i}$	$\frac{\text{degree}}{\text{degree}}$	-0.700	-0.634
$\left(\frac{\Delta Z_i}{\Delta t'_i}\right)_{\delta_i}$	"	+0.904	-0.019
$\left(\frac{\Delta R}{\Delta t'_i}\right)_{\delta_i}$	$\frac{\text{km}}{\text{degree}}$	-3.10	+2.90
$\left(\frac{\Delta R_i}{\Delta t'_j}\right)_{\delta_j}$	"	+3.06	-3.28
$\left(\frac{\Delta h_i}{\Delta t'_i}\right)_{\delta_i}$	"	-3.12	+2.72
$\left(\frac{\Delta h_i}{\Delta t'_j}\right)_{\delta_j}$	"	+2.99	-3.11

The error involved in reading the globe scale should not exceed 0°.2. For fast meteors with a high apparent angular velocity and with a common point of only moderate quality, say 2, the common-point error would be about 1°. We believe this to be considerably greater, perhaps by a factor of 2, than the common-point error for the average meteor. Positioning errors can occur in two ways. First, the two films may not be properly superimposed. Because the globe is not perfectly spherical and because its mean radius is not exactly that of the films, we can not always superimpose the entire star field common to both films. The attempt is always made to carry out the superposition in the vicinity of the meteors and an error of about 0°.5 would probably be large. The second positioning error, resulting from an unknown time of the meteor occurrence, is a special case and will be treated separately.

From the preceding extreme figures, we may estimate that the average error, in t_1 or δ_1, will almost certainly not exceed 1°. It is unfortunate that this figure cannot be verified by more rigorous methods than those used. However, another check on our errors, to follow later, will supply additional information tending to confirm this as being an extreme value.

Let us assume that the common point at Station B has been properly located, positioned and measured, and that, for any of the aforementioned reasons, a 1°.0 error exists

in the measures of the common point at Station A. The percentage errors for this case, computed from the quantities in Table 7, are given in Table 8.

Table 8

Errors Resulting from a 1°.0 Error in the Common Point

Percentage Error in:	$\Delta\delta_A = 1°.0$	$\Delta t'_A = 1°.0$
R_A	3.7%	3.6%
R_B	3.7	3.7
h_A	3.5	3.7
h_B	3.8	3.7

The similarity of values within either column should be expected. The similarity between corresponding values of the two columns is the result of chance and indicates that the maximum error for the meteor will occur for departures in a direction roughly half way between the directions of the δ and the t axes.

When the instant of the meteor is unknown, we choose the time of the middle of the exposure for reduction purposes. Thus, with 12-minute exposures our maximum error is $\Delta t = 6$ mins = 1°.5. However, in this case the common points do not suffer a shift relative to one another and the resulting errors in the ranges will be the algebraic sums of the errors caused by the displacement of both common

points. Since these are of opposite sign and of about the same magnitude (see Table 7), the final errors will be small. Table 9 shows the percentage errors resulting from a 1°.5 shift in t of both films.

Table 9

Errors Resulting from a Displacement of $\Delta t = 1^{\circ}.5$ of Both Films

Quantity	R_1	R_2	h_1	h_2
Error (km)	+0.34	-0.14	+0.20	-0.17
Percentage Error	0.4	0.2	0.2	0.2

We can see that the timing error will be negligible even in those cases where the maximum possible error results from a displacement along the t-axis.

G. Velocity Errors

Errors in velocity may result from errors in any of the measures. Errors in the apparent angular velocity, ω_1', are probably small compared to any other type and we will neglect these. From differentials of equation (43) we see that the percentage errors due to range and radiant errors are, respectively:

$$\left(\frac{\Delta v}{v}\right)_{\omega', R} = \frac{\Delta R}{R}, \text{ and} \tag{58a}$$

$$\left(\frac{\Delta v}{v}\right)_{\omega', R} = -\cot r \, \Delta r. \tag{58b}$$

Thus the error in velocity cannot be less than the range error, which we found to be about 4 percent with the assumption of a common point error of 1°.0. The function Δr is itself a function of r as one can understand by visualizing the extreme cases when the meteor appears at the radiant ($r = 0°$, $\Delta r = 0°$), and when the meteor appears at a great distance from the radiant (say, $r = 90°$, $\Delta r = ? \neq 0°$). We might estimate this unknown Δr to be of the order of 5° or 10° in the worst cases. We may say that certainly Δr varies less rapidly than tan r. This leads to the apparently contradictory result that, in general, meteors must have a badly determined radiant to allow us to produce an accurate velocity. However, another independent error in r, that imposed by our scale reading accuracy, 0°.2, weighs more heavily against meteors of small r. These two errors may combine in such a way that meteors at some intermediate r give the best velocities.

We have no method of determining a satisfactory relationship between r and Δr and we must therefore approach this problem from another side. Among the meteors reduced, there are 36 Orionid and 45 Geminid shower meteors for which we know velocities. These groups will determine our velocities errors. Furthermore, since most meteors in these showers were reduced by both the direct and indirect methods, we can find some estimate of a criterion for choosing between the results of the two methods.

In general, the direct velocities derived from the two films of a given meteor do not agree with one another to within several percent. However, in some examples, the radiant distance of one common point greatly exceeds that of the mate plate and in these instances, the velocity derived from the more distant trail was used or weighted more heavily in the average. Average velocities, mean errors and percentage errors were found for both sets of shower meteors for the following cases:

(a) Direct velocity used for all meteors.

(b) Indirect velocity used for all meteors.

(c) Indirect velocities used when $|B| \geq 10°.0$, direct when $|B| < 10°.0$.

(d) Same as (c), with division made at $|B| = 9°.0$.

(e) Same as (c), with division made at $|B| = 8°.0$.

Table 10 gives the average values, mean deviations and percentage errors for each of these velocity criteria and for both groups of shower meteors. The letters refer to the outline above.

Table 10

Mean Values and Errors of Shower Meteor Velocities

(For description, see text)

	Number of Meteors	Number of indirect determinations used	$\bar{V}\left(\frac{km}{sec}\right)$	$\sigma\left(\frac{km}{sec}\right)$	% error
Geminids					
(a)	44	0	35.7	1.42	4.0%
(b)	38	38	35.7	1.74	4.9
(c)	45	16	36.3	0.92	2.5
(d)	45	21	36.1	1.05	2.9
(e)	45	26	36.0	1.13	3.1
Orionids					
(a)	34	0	68.3	3.01	4.4%
(b)	34	34	67.2	2.52	3.8
(c)	36	18	68.2	2.59	3.8
(d)	36	24	67.7	2.17	3.2
(e)	36	28	67.6	2.05	3.0

We should qualify these data before discussing the results. First, the Geminids were somewhat brighter meteors than normal and, hence, easier to measure. Furthermore, the radiant of this shower is not far distant from α Geminii, a star that appears on most of the Geminid meteor photographs. Since these meteors were reduced specifically to check for errors, it was necessary for the measurer to "forget" the position of the radiant for each measure, a difficult task with a radiant so clearly marked. Still, we believe this was accomplished.

In the case of Orionids, the situation is quite different. The radiant was not present on the region being photographed and, more important, we did not realize we were reducing

shower meteors until after the measures had been completed. Also, these meteors did not produce such bright trails as the Geminids. Perhaps, then, the Orionids should be regarded as giving the best test, although, as can be seen in Table 10, the errors for both showers are comparable.

In regard to the indirectly determined velocities, our measured quantities are A and B as defined by equations (46) and (47). It may easily be shown that if the radiant is properly chosen and there are no measuring errors, then

$$\Delta r_A = \Delta r_B = \frac{(\Delta A + \Delta B) \sin^2 r_+}{\sin B} \qquad (59)$$

where r_+, is the angle from the radiant to the common point of the trail most distant from the radiant. A poorly determined common point has little effect on A, since this quantity is determined from a ratio of the ranges, R_1/R_j. We have already seen that a reasonable error in the common point results in comparable changes, of the same sign, in the two ranges. We may write:

$$A \sim \frac{R_A}{R_B}. \qquad (60)$$

Differentiating this equation, we obtain

$$\Delta A = \frac{R_B \Delta R_A - R_A \Delta R_B}{R_B^2}. \qquad (61)$$

Thus, the errors in the range tend to compensate one another in the determination of A. However, since we must still apply the velocity equation (43) in its original form after determining r_1, any error in range will affect the velocity in the usual fashion.

One can see that an error in the common point will directly effect B which is essentially the distance between common points. It is also clear from the $\frac{1}{\sin B}$ factor in equation (59) that the indirect method will be more powerful when |B| is sufficiently large. From the shower meteors we can obtain an idea of how large.

Table 10 indicates that the deviation from the mean velocities of the showers is of the order of 3 to 4 percent, but we have yet to show that these mean velocities actually correspond to those expected for these showers. Our velocities are those at some point in the atmosphere, uncorrected for deceleration and therefore somewhat lower than the usually quoted velocity outside the atmosphere. In general, we choose common points as near the beginning of the trail as possible to minimize the deceleration correction. From Orionid and Geminid meteors reduced by Jacchia, we have obtained the velocities at the beginning point of the meteor. (v_o). These results, as well as Jacchia's values for the no-atmosphere velocity (v_∞) are given in Table 11. They are compared with the average velocity we obtained for the method which yielded the smallest σ in Table 10.

Table 11

Average Velocities of Shower Meteors Obtained

by Accurate Reductions

(By Jacchia)

	No. Meteors	v_∞	v_o	v_{REM}
Geminids	17	36.6	36.3	36.3
Orionids	7	67.5	67.4	67.6

The agreement is excellent and there is no evidence for a systematic error with velocity. We may conclude that our velocity errors, for these cases, are about 3 percent, and that the optimum minimum value of |B| for the indirect reductions is about 8° to 10°. It seems unlikely that measures on somewhat shorter and fainter non-shower meteors would yield errors that exceed 5 percent. When this result is compared with the errors expected for ranges and heights, we see that we must have over-estimated the probable error in the common point, for as was pointed out earlier, the velocity error cannot be less than the range error, which was of the order of 4 percent on the assumption of a 1°.0 error in common point.

There still remains the possibility that in selecting the shower meteors, we passed over some cases which were so badly determined that they were unrecognizable as members of the shower. A study of the frequency diagram of the

velocities of the individual meteors makes such a hypothesis unlikely if, on the basis of such a diagram, one is willing to grant that the scatter may be represented to a fair degree of approximation by the usual error curve. We have reproduced in Figure 5 the frequency diagram for the directly determined velocities of our Geminid meteors.

Figure 5

VELOCITY DISTRIBUTION OF GEMINID SHOWER METEORS, APPROXIMATE REDUCTIONS

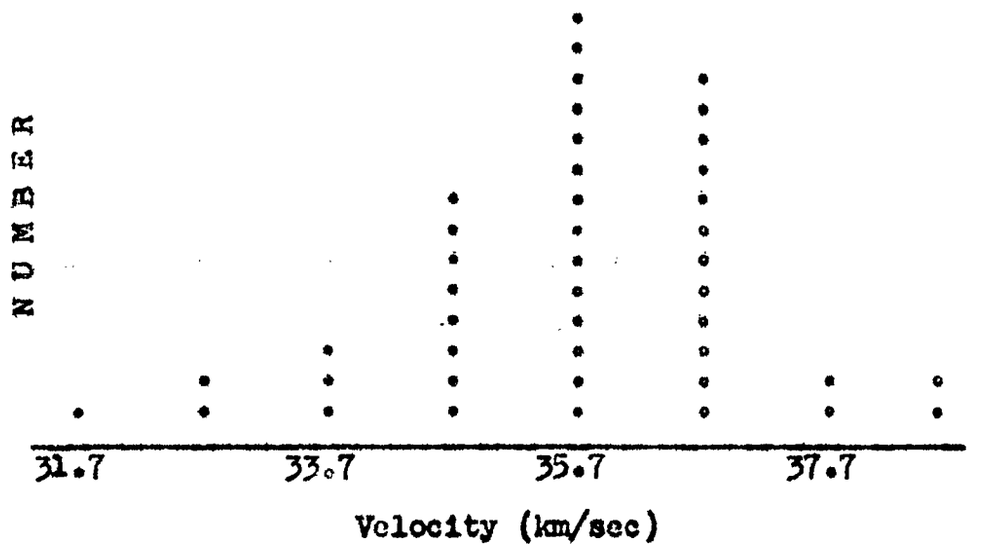

H. Some Specific Results of the Approximate Reduction Method

In selecting meteors for approximate reductions, we inspected every meteor film, in chronological order, to determine whether it was possible to make a reduction. We discarded as few meteors as possible, and would have preferred to exclude no meteors, so that the over-all statistics would be unassailable. However, some individual cases clearly would have yielded results of very poor quality. About 15 percent of the meteors were in this category, and rejected for one of the following reasons:

(a) The meteor was too faint or too short for the radiant to be determined.

(b) The difference in image quality (focus or fog) of the mate films was such that no satisfactory common point could be found.

A further fifteen percent of the meteors were also discarded because their geometry or positions made reductions impossible or difficult. These included:

(c) Meteors so close to the radiant on both films that the photographic spreading of the image obscured the breaks.

(d) Meteors that appeared on the film only in part and, as a consequence, could not yield a satisfactory common point. Not all such partial meteors were excluded, however, since in many cases a good estimate of a common

point could be made.

In addition, another fifteen percent of the meteors photographed were not available for reduction at the time of this study. They include:

(e) Meteors being reduced in the accurate reduction program. These, in general, are brighter than those we have treated. Their exclusion is responsible for the homogeneity, with respect to brightness, of our meteors.

(f) Other meteors occurring on the films included in (e). These, we suppose, are a random selection in all respects.

Of the remaining 55 percent which we reduced, we later discarded from the statistics a very small fraction of a percent, because large discrepancies in the final results indicated that a solution was too difficult.

At present (November, 1955), data are available for about 1600 meteors, photographed from the beginning of the double-station Super-Schmidt program, February, 1952, through February, 1954. Present plans call for a total of at least 2000 meteors photographed over a period of at least two years.

The data we wish to present here do not include all that are available. The results quoted in the remainder of this thesis are based on all the reductions that had been

completed at the time the particular analysis was made. This will explain the varying number of meteors we include in attacking the several aspects of this study.

To begin with, we shall mention briefly the distribution of meteor velocities. Although we wish to divorce this aspect of the data from the general subject of the thesis and to treat it separately in a later paper, we shall need to refer to the distribution when discussing fragmentation phenomena. Table 12 summarizes the data on the first 1069 meteors to be reduced. Included are meteors occurring between February 1952 and June 1953. For comparison we have also listed the early information, compiled by Whipple (1954), obtained from the small camera meteors. His velocities are those at the top of the atmosphere, v_∞, and ours at the measured common point nearest the beginning of the trail. The slight correction for deceleration necessary to make the two groups strictly comparable is very small compared to the 10 km/sec sub-groups we have chosen. We have also listed the distribution of all meteors, expepting the Perseid, Orionid, and Geminid showers, which add an appreciable number to either the present or to Whipple's total. Whipple lists a total of only 51 sporadic meteors and consequently the elimination of <u>all</u> shower meteors leaves few for comparison.

Table 12

Velocity Distribution of 1069 Super-Schmidt Meteors Compared with the Distribution of 144 Small Camera Meteors

(See Text for Classifications)

v km/sec	Percent of Total for Cases:				
10-15	13.7 %	14.8 %	3.5 %	4.5 %	3.9 %
15-20	16.5	17.8	6.2	8.1	15.7
10-20	30.2	32.6	9.7	12.6	19.6
20-30	22.7	24.6	24.3	31.5	27.5
30-40	21.0	18.2	30.6	22.5	15.7
40-50	6.5	7.1	6.9	9.0	3.9
50-60	9.8	5.2	5.6	5.4	9.8
> 60	14.8	12.3	22.9	18.9	23.5

The five categories of meteors listed in the table include the following:

(a) 1069 Super-Schmidts, representing all those occurring between February, 1952, and June, 1953, and reduced by approximate means.

(b) 988 meteors remaining from (a) after the exclusion of all meteors in three major showers (45 Geminids, 36 Orionids, 0 Perseids).

(c) 144 small camera meteors by Whipple (1954).

(d) 111 meteors remaining from (c) after the exclusion of all meteors in three major showers (19 Geminids, 2 Orionids, 12 Perseids).

(e) Those meteors (51) in (c) that are sporadic.

Regardless of which categories of meteors we compare, we see that the older data rather badly underestimated (or we have overestimated) the number of meteors in the lowest velocity group. It may be that the explanation lies in the choice of meteors accepted for accurate reduction. Meteors of low apparent velocity may have the shutter breaks greatly obscured by photographic diffusion of the dash image, so that the meteors are difficult or impossible to measure. Such cases would be selectively rejected, leaving a preponderance of faster meteors.

Statistics concerning phenomena apparently caused by fragmentation of the meteor are available for 585 cases, all the meteors occurring between February and December, 1952. For each of these meteors we have recorded the presence and position of wake and terminally blended dashes. The wake, in the best examples, is seen as a trail of steadily decreasing luminosity extending from a dash towards the direction of the radiant. When the wake is strong, the image due to both dash and wake may assume a tear-drop shape. In more usual cases one can only notice that the dash lacks symmetry in the direction of the meteor's motion. For faint photographic meteors, one cannot be more explicit in describing the appearance of wake.

Terminal blending, in the strict sense, is a term that should be reserved to describe those dashes that do not necessarily show an asymmetry but are longer than the

expected one-fourth of a shutter cycle. Often the final images will be very faint but will clearly be more diffuse than some earlier images. We cannot always decide whether such an image should be designated as wake or as terminal blending. We generally classified such cases as blending. Although this represents a consistent approach, the result has probably been to overweight the occurrence of blending by an appreciable amount. Good examples of wake are certainly more common than good examples of terminal blending and perhaps one should expect the same to be true for the poorer examples. By expressing some doubt concerning the number of meteors displaying <u>each</u> of these characteristics, we do not wish to imply a question as to whether any of these meteors displayed <u>one</u> of the fragmentation phenomena.

In 1954 we made a preliminary study of the correlation of the visible effects of fragmentation and velocity, on the basis of some 50 faint meteors. The analysis of the 585 meteors confirms the conclusion that the existence of wake and of terminal blending are both a function of velocity. Table 13 lists the results.

Table 13

Percentage of Meteors in Various Velocity Groups that Display Some Visible Effects of Fragmentation

v (km/sec)	Wake	Terminal Blending	Wake and Terminal Blending	Wake and/or Terminal Blending
10-15	32%	79%	23%	89%
15-20	41	53	25	69
10-20	37	63	24	77
20-30	39	30	11	57
30-40	29	32	16	44
40-50	25	9	3	31
50-60	10	8	3	15
>60	12	3	1	14
ALL	28%	30%	12%	45%

For the reasons given above, the final column of Table 13 should be considered to be the best set of data; it gives the percentage of meteors in the given velocity groups that show wake or terminal blending, or both.

These figures agree in a general way with those obtained by Jacchia (1954) for a group of 137 bright Super-Schmidt meteors. He found wake in 46 percent of the cases, terminal blending in 34 percent, both in 16 percent, and either in 61 percent. The higher percentages are the result of his greater average meteor brightness. Jacchia notes that all meteors of maximum apparent brightness of more than four magnitudes above plate limit show some wake. The indication is that all meteors release some wake particles and when the

meteor is large enough, the total intensity of all the particles will be great enough to register on the emulsions. A velocity dependence was also seen in these meteors in the sense that the wake was brighter among the low-velocity meteors than among high-velocity meteors of the same apparent magnitude.

A considerable discrepancy exists between the velocity dependences of terminal blending in the two sets of data. Jacchia found none, but ours is most pronounced. This is probably explained in part by our choice of the terminal blending category for doubtful cases. In addition, a selection factor, to be discussed in Chapter III, in Jacchia's choice of meteors seems to affect his result.

We will, from time to time, introduce more statistical data derived from meteors treated by the approximate techniques.

CHAPTER III

BEGINNING POINTS OF METEORS

A. Meteors Characterized by an Abrupt and Early Rise to Maximum Light

Certain faint meteors display a light curve that may best be described as "backwards". In the most extreme cases the meteor appears at maximum light, rising 1.0 or 1.5 magnitudes above plate limit within the period of time between the dashes (1/80 sec); it then becomes progressively fainter. The light curve, measured in magnitudes, on the declining branch is almost linear in time. The final breaks show terminal blending. By reversing the time scale, one can obtain a very plausible representation of the light curve of a normal high-velocity meteor.

In less extreme cases, these meteors may appear at an intensity close to the plate limit and show a normal increase in brightness for several dashes followed by a more or less abrupt rise to a maximum where the change in brightness may be abrupt or smooth. As before, terminal blending is likely to be present in the final dashes.

There are no examples of this form of light curve among any of the several hundred larger meteors photographed on small cameras. Abrupt meteors are apparently peculiar to those smaller objects that can be photographed only with

Super-Schmidt cameras.

Of all the meteors photographed in the first year of the Super-Schmidt double-station program (February, 1952 to February, 1953) and reduced by our approximate method, 13 percent of the meteors could be assigned to this category. Although the observational data clearly demonstrate the existence of a class of abrupt meteors, some examples occur that are hard to classify for one or several reasons: (a) the rise is steeper than normal but not abrupt, (b) the increase in light is noticeable but not great, (c) the light curve falls off rapidly at some point after the rise in such a way that the abnormality might be described as simply a prolonged flare, (d) the discontinuity of the light curve occurs so late in the trail that only a small fraction of the meteor departs from normality, or (e) the meteor shows a mixture of the above effects. We have relied entirely on our subjective appraisal of each case in deciding whether a given meteor should be included in the class of abrupt meteors.

The information derived from the approximate reductions indicate that at least three other qualities are shared, statistically, by such meteors. First, as in the case of wake, abrupt meteors are characteristically a low-velocity phenomenon; nearly a third of all meteors of velocities less than 20 km/sec fall into this class (Table 14).

Table 14

Velocity Distribution of Abrupt Meteors

v ($\frac{km}{sec}$)	No. reduced Feb., 1952- Feb., 1953.	No. Abrupt Meteors	% Abrupt Meteors
10-15	85	27	32
15-20	105	31	30
20-30	151	22	15
30-40	185	11	6
40-50	49	3	6
50-60	47	1	2
> 60	140	5	4
Total	762	100	13%

Second, abrupt meteors are, in general, short in duration. Since the meteors in this study represent a rather homogeneous group with respect to their maximum magnitude, we would expect a homogeneity in the durations of any given velocity group unless some distinction in the physical processes exists between different types of meteors. Table 15 lists the median and mean number of dashes observed for (a) all normal meteors; (b) normal meteors with velocities less than 20 km/sec, and (c) all abrupt meteors.

Table 15

Comparison of the Durations of Normal and Abrupt Meteors

		All Normal Meteors	Normal Meteors, v< 20 km/sec	All Abrupt Meteors
No. of Meteors		380	89	100
No. of Dashes	Median	19	23	16
	Mean	23.0	28.8	17.7

The mean values are heavily influenced by a few bright meteors, none of which show an abrupt rise. The median values of the low velocity meteors probably should be used as the standard for comparison, since over two-thirds of the abrupt meteors have velocities in this range. However, any comparison of figures in Table 15 shows a significant decrease in the duration of abrupt meteors.

Finally, terminal blending was detected in about two-thirds of the abrupt meteors and was strongly concentrated among the lower velocity objects. Furthermore, if we describe the blending qualitatively in terms of the number of dashes for which terminal wake was recorded, the velocity effect is even more pronounced. (See Table 16).

Table 16

Extent of Terminal Blending Among Abrupt Meteors as a Function of Velocity

	$v < 20$ km/sec	$v \geq 20$ km/sec
Percent of abrupt meteors with terminal blending	83%	34%
Average number of breaks with terminal blending among abrupt meteors	5.6	1.3

The preceding table and short duration of abrupt meteors supply, in part, an explanation for the discrepancy between our results and those obtained by Jacchia in the case of the velocity dependence of terminally blended meteors. To measure decelerations, meteors of great length are preferred. The very short abrupt meteors are not suitable and they have probably been selectively rejected for purposes of accurate reduction. However, these meteors are just those which show a strong velocity dependence in the terminal blending characteristic.

The various anomalies of these meteors have in the past, Jacchia (1954), McCrosky (1955), been very logically explained as the result of a sudden crumbling of the meteoroid at the point of the abrupt rise. The resulting increase in the effective surface area causes the increased luminosity. Differential deceleration of fragments of different sizes causes the mass of the original meteoroid

to spread along the trail and obscure the shutter breaks. The duration of the meteor will be that of the largest fragments and not that of a single body and consequently the meteor will not endure. The qualitative data of this study have not produced a result at variance with this description of the phenomenon. Moreover, we will be able to make the crumbling-hypothesis still more plausible by a quantitative statistical study.

We may describe these abrupt meteors in terms of a relatively few observational parameters. The degree of crumbling, as measured by the increase of the effective area, is proportional to the luminosity before and after the discontinuity. It can be seen that in a general way the slope of the rising branch of the light curve is related to the rate of crumbling; and the duration and slope of the declining branch is, in some complex fashion, dependent on the distribution of particle sizes after crumbling. The brightness and degree of the terminal blending are also related to this distribution. The height at the point of disruption, the velocity, and the angle of approach into the atmosphere complete the list of the important quantities that may be obtained without recourse to the accurate reduction methods.

Unfortunately, one of the most interesting pieces of information is not available in many of the cases studied. Very often the meteor shows no image before the steep rise

and we can only fix an upper limit on the effective area of the body before fragmentation. This upper limit is set by the limiting magnitude of the film, which is itself a function of the length of the dash (a long and faint dash can be as easily detected by eye as a shorter but brighter dash). Since the dash length depends on velocity, we will introduce an extraneous velocity dependence on the intensity increase, ΔI, in the sense that the larger values of ΔI will occur for higher velocity meteors. Even in those cases where the meteor shows several faint dashes before the burst, the value of ΔI may be in error by an amount corresponding to 0.3 or 0.4 magnitudes because of the difficulty of estimating the brightness of low-intensity images.

We are in a better position with respect to height. The common point is extremely well determined because of the discontinuity in the light curve. The velocities, too, should be of good quality in so far as they depend on the ranges. Of course, these meteors are short and the determination of the radiant distance, r, by the direct method is somewhat less reliable.

If the assumption of rapid crumbling of the meteor is valid, we might expect the disruption to occur because of an internal explosive phenomenon or because of crushing caused by external pressure forces. We might also include the possibility that gross fracturing occurs as a result of a temperature differential through the

meteoroid. We believe that the abrupt meteors supply us with good evidence that the crumbling occurs when the dynamic pressure, ρv^2, on the body surpasses the crushing strength of the meteoric material.

Values of the air density, taken from the Rocket Panel Atmosphere (1952), were found for the bursting heights of 74 excellent cases of abrupt meteors. It was assumed that these heights could be related to the meteor velocity by an equation of the form:

$$\rho v^n = C \tag{62}$$

or

$$\log \rho + n \log v = \log C. \tag{63}$$

A least-squares solution was applied to find the constants. These values are compared, in Table 17, with the results of similar least-squares solutions for the densities at the beginning heights of normal meteors. We have also quoted the correlation coefficients, R, for the best values of $n = n_o$ and for other values of n. The relatively low probable error for the solution comprising the 74 abrupt meteors is probably indicative of the increased accuracy resulting from reductions of meteors with well determined common points.

Table 17

Least-Squares Solution of Equation (63) for Beginning Points of Normal Meteor and for Bursting Points of Abrupt Meteors

	Abrupt meteors	All normal meteors	Normal meteors, $v < 40$ km/sec
No. of meteors	74	238	142
log C (cgs)	4.10	9.42	
n_o	1.94 ± 0.11	2.82 ± 0.07	3.11 ± 0.14
R	$0.84 \pm .03$	$0.91 \pm .01$	
n	1.0	2.0	
R	$0.74 \pm .05$	$0.87 \pm .02$	
n	3.0	4.0	
R	$0.71 \pm .06$	$0.83 \pm .02$	

The normal meteors used for comparison were the first group of meteors to be reduced. Additional data are available at this time but have not yet been utilized in a least-squares solution. Such work will not be carried out until after the approximate reduction program has been completed, and after a study of errors has been made by the comparison of a larger number of cases treated by both the accurate and the approximate systems of reduction.

However, the probable errors leave no doubt that the beginning points of these faint normal meteors occur according to a law different from that obeyed by the bursting points of abrupt meteors.

By selecting only the excellent cases of meteors with abrupt rise, we gain the double advantage of using the meteors with the most accurately known heights, and of limiting our material to a group of meteors that indisputably belong to the same class. In this process we are neglecting about 25 percent of our data and are also reducing the range of velocities and heights since, as we have mentioned, the best examples of abrupt meteors are low-velocity objects. This latter fact suggests that possibly the ρv^2 = constant law approached by abrupt meteors is a result solely of their velocity. However, a study of low velocity normal meteors (see Table 17) shows that only a small change in the velocity exponent occurs for these meteors as compared to that for normal meteors of all velocities.

Figure 6 shows the relationships determined for the beginning heights of normal meteors and the bursting heights of abrupt meteors as functions of velocity. The filled circles represent individual cases of the beginning points of normal meteors and the open circles represent the bursting points of abrupt meteors. In spite of the wide

Figure 6

ATMOSPHERIC DENSITIES AT BEGINNING AND BURSTING POINTS VERSUS METEOR VELOCITIES

Beginning points of normal meteors and least-squares solution for ρv^{n} = constant.

Bursting points of abrupt meteors and least-squares solution for ρv^{n} = constant.

Point of disruption of 7 meteors showing a hump in the light curve (data from Jacchia).

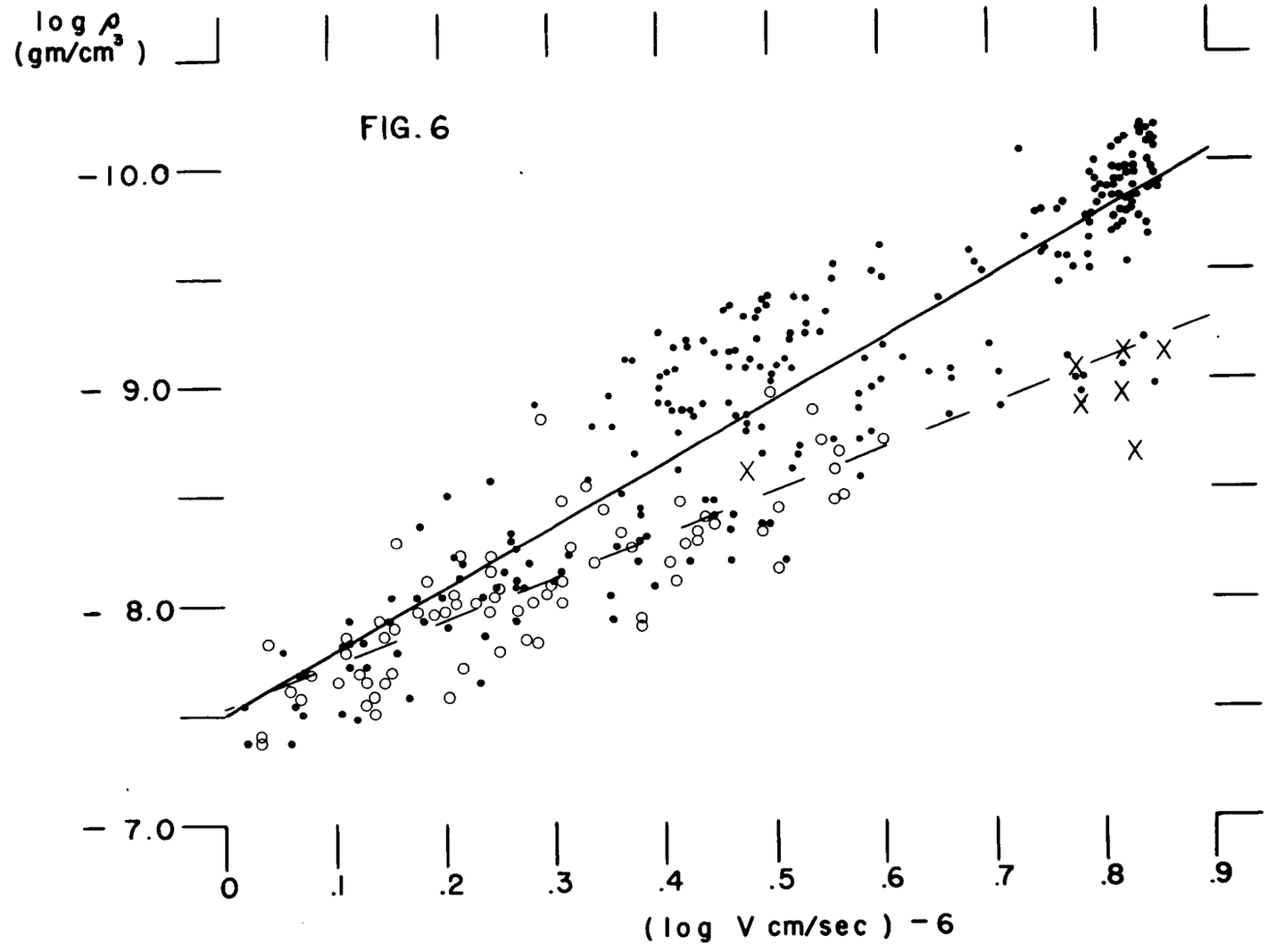

FIG. 6

scatter, most of which is probably real, one can readily see the distinction between the two groups.

Tracing the course of the average meteor by means of this graph, we see that it first reaches a point in the atmosphere at which it may be expected to become luminous. That is, on the classical meteor theory, heat transfer to the body becomes sufficient to vaporize the material. Then at some later time, which depends on the meteor velocity, the pressure on the body (ρv^2) exceeds the crushing strength of a certain class of meteoroids and the abrupt rise in intensity may occur. The scatter that is possible in these points may cause any given meteor, especially if it be a low-velocity object, to be visible first at the fracturing point. However, for high velocity meteors our results predict that in almost all cases the burst will not occur at the beginning point of the meteor. A confirmation of this, and of the result in general, is supplied by seven meteors studied by Jacchia (1949). These meteors showed an unusual increase in luminosity on the rising branch of the light curve. This behavior is abnormal in contrast to the flaring meteors as described by Miss Hoffleit (1933) and Jacchia. Both found flares to occur later in the meteor's trajectory. Also, unlike a true flare, the luminosity of these seven meteors remained high after the burst and did not retreat to the level predicted by the

theoretical light curve. Jacchia tentatively associated this phenomenon with the atmospheric E-layer but it seems certain now that the correlation was due to chance. We have plotted the disruption points (X's) for these meteors in Figure 6. Their agreement with the constant pressure curve is good.

B. Beginning Points of Normal Meteors

Our interest in normal meteors in the preceding section was induced primarily by our desire to compare them with the special class of abrupt meteors. However, the result obtained is worth further study and explanation, even though only an approximate approach is feasible at this time.

First, we should point out explicitly that the beginning point is a function of the instrument as well as of the meteor. It is the first dash image of sufficient intensity to be photographed and detected by eye on a careful inspection of the trail. Often the observer will be able to detect a questionable image (or images) at a point before the first well defined dash. The beginning point of such a meteor may be in error by that amount if the observer incorrectly decides that the doubtful images do or do not belong to the meteor trail.

We will ask how our observed distribution of beginning points as a function of velocity agrees with the predictions of the meteor theory.

The intensity at any point, given by equations (6b) and (7a), is

$$I = -\frac{\tau_0}{2}\dot{m}\,v^{\mu} \tag{64}$$

where

$$\dot{m} = -\frac{\Lambda}{2\zeta} A\,\delta_m^{-2/3}\,m^{2/3}\rho v^{\nu}.* \tag{65}$$

We have replaced the exponents, 3, by the general quantities, μ and ν. Our result will consist of one equation involving these two unknowns. We have then, the relationship:

$$I \sim m^{2/3}\rho v^{\mu+\nu}. \tag{66}$$

---

* Strictly speaking, we should consider both Λ and ζ as functions of velocity. In the case of Λ, we can only make a negative statement: there is no reason to believe it remains constant.

For ζ, we could refer to the theoretical reaction rate model proposed by Cook, Eyring and Thomas (1951). Under such a hypothesis, higher velocity meteors may acquire energy at such a rate that the surface would be maintained at a temperature in excess of the vaporization temperature. The energy per gram of mass lost would then exceed that determined by the latent heat.

We shall, however, neglect these changes and base our calculations on the classical meteor theory, utilizing $\frac{\Lambda}{\zeta}$ = constant.

From our previous result, we know the relationship between ρ and v for average normal meteors. Supposedly, we can find a similar relation for I and v for these meteors. If, then, we can do the same for the masses, we will be able to check the functional representation given by equation (66). To find accurate meteor masses, we must rely upon accurate photometry of the entire meteor trail and the use of equation (10),

$$m_\infty = \frac{2}{\tau_0} \int_{-\infty}^{\infty} \frac{I\, dt}{v^\mu} \qquad (67)$$

Neglecting any change of velocity, we have:

$$m_\infty v^\mu = \frac{2}{\tau_0} \int I\, dt. \qquad (68)$$

Jacchia (unpublished) has devised an approximate method for determining the integrated intensity, which we will reproduce here.

Let I_{max} be the meteor intensity at the point of maximum light and I_{lim} the limiting intensity of the plate. We define

$$\Delta M = M_{lim} - M_{max} = -2.5 \log \frac{I_{lim}}{I_{max}} \qquad (69)$$

Also, let T, the duration of the meteor, be defined as the time during which the meteor intensity is above the plate limit.

We will employ a gaussian curve to represent the intensity of the meteor as a function of time:

$$I = I_{max}\, e^{-h^2 t^2}. \qquad (70)$$

We have chosen the time scale such that $I = I_{max}$ at $t = 0$. Then $I = I_{lim}$ at $t = \pm \frac{T}{2}$. It follows that:

$$I_{lim} = I_{max}\, e^{-h^2 \frac{T^2}{4}}, \qquad (71)$$

and

$$h = \frac{2}{T}\left(\ln \frac{I_{max}}{I_{lim}}\right)^{1/2}. \qquad (72)$$

From equation (69) we then find,

$$h = \left(\frac{3.034}{T}\right)\left(\frac{\Delta M}{2.5}\right)^{1/2} = 1.919\, \frac{(\Delta M)^{1/2}}{T}. \qquad (73)$$

We can now integrate the intensity, as:

$$\int_{-\infty}^{\infty} I\, dt = \int_{-\infty}^{\infty} I_{max}\, e^{-h^2 t^2} dt = .924\, \frac{I_{max}\, T}{(\Delta M)^{1/2}} = \frac{\tau_o}{2}\, n_\infty\, v^4; \qquad (74)$$

The use of the gaussian may be questioned. For low-velocity meteors, the representation may be very good. For high-velocity meteors, whose light curves are not symmetrical, it can be very bad. However, the integrals under the gaussian, as defined, and under the actual curve do not differ greatly. In this case, the proof of this pudding lies in the result of comparing the accurately integrated

intensities and the approximately integrated intensities. Jacchia finds the agreement to be extremely good (~5 percent) in those examples for which a comparison was made.

As a result of equation (74), we may compute the quantity, $m_\infty v^\alpha$. The duration is given in terms of the total number of breaks visible, N. M_{max} (or I_{max}) is obtained from photometry (see Jacchia, 1949). To determine M_{lim}, we assume that the magnitude of the meteor at the beginning point is that of the plate limit, where the plate limit is defined as the magnitude of the faintest star visible on the photometric comparison plate possessing star trails of the same length as the meteor dash. G. S. Hawkins (unpublished) has kindly supplied us with his estimates of these values, given as a function of the length of the star images. The estimates are considered accurate to within 0.2 magnitudes.

Although we lack precise photometry on meteors treated in this work, we do have a group among those used in the beginning point determination for which consistent, if not absolute, estimates of maximum magnitude have been made. Using equation (74) we have determined the integrated intensity of 111 such meteors. The average values of the logarithm of this quantity, as a function of velocity class appears in Table 18.

Table 18

Average Integrated Intensity of 111 Meteors as a Function of Velocity

Velocity class (km/sec)	10-20	20-30	30-40	40-50	50-60	>60.	all
Number of meteors	28	28	17	12	9	19	111
log $\int I\,dt$ in arbitrary units	.83	.90	.83	.96	1.19	.80	.87

The scatter in the individual value of log $\int I\,dt$ is considerable but there is apparently very little velocity correlation. A least-squares solution for the exponent in the equation

$$v^n \int I\,dt = \text{constant} \qquad (75)$$

yielded

$$n = -0.1 \pm 0.1.$$

We have, then,

$$m_\infty v^\mu \approx \int I\,dt \approx v^{0.1 \pm 0.1} \qquad (76)$$

or

$$m_\infty \approx v^{(-\mu + 0.1) \pm 0.1}. \qquad (77)$$

Since a negligible amount of material has been lost by the meteor by the time it first become visible, we may assume $m_\infty = m_0$.

For information relating to the intensity at the beginning point, we shall consider a group of "average" (to be defined) meteors. We shall assume, as we did in determining the integrated intensity, that the magnitude of the first visible dash is equal to the limiting magnitude of a comparable trailed comparison plate. To convert this to absolute intensity we must make several assumptions, listed below. The numerical values derived from these assumptions will define the average meteor. We assume:

(a) The average distance of the meteor from the radiant, in terms of sin r, is the same for meteors of all velocities. From the average of 100 meteors we determined an average value of $\overline{\sin r} = 0.58$.

(b) The average zenith distance of the beginning point of the meteor, in terms of cos Z, is the same for meteors of all velocities. For the same meteors used in (a), we found this average to be $\overline{\cos Z} = 0.94$.

Table 19 lists the various steps in the correction of the beginning magnitudes (apparent) to units of absolute intensity. The computations are made for 7 average, and hypothetical, meteors with velocities between 10 and 65 km/sec. Rows 2, 3, and 4 give respectively, the density (ρ) at the beginning point, computed from equation (63) and Table 17; the corresponding height above sea level (H) as taken from the Rocket Panel Atmosphere, and the height above the point

of observation (h). Using the average value of cos Z, we obtain the range, R, from equation (39):

$$R = \frac{h}{\cos Z} = \frac{h}{.94}. \qquad (78)$$

From equation (44), we may now determine the length of the meteor dash for each of these velocities, by using the value, $\overline{\sin r} = 0.58$ found above. We may write,

$$v = \frac{\omega' R}{\sin r}$$

or

$$\frac{\omega'}{4} = \text{dash length} = \frac{v \sin r}{4 R}.$$

Row 6 contains the limiting apparent photographic magnitudes for dashes of this length, as interpolated from Hawkins' values. In row 7, M_p', we have corrected the preceding value for the difference of the trailing velocities of comparison star and meteor, and row 8 is the absolute photographic magnitude; that is, the magnitude the beginning point would display had it been at 100 km distance.

The plot of log I against log v (see Figure 7) gives a graphical solution to the velocity dependence of the intensity at the beginning point of the normal meteors. We find that

$$I \approx v^{.69 \pm (?)}. \qquad (79)$$

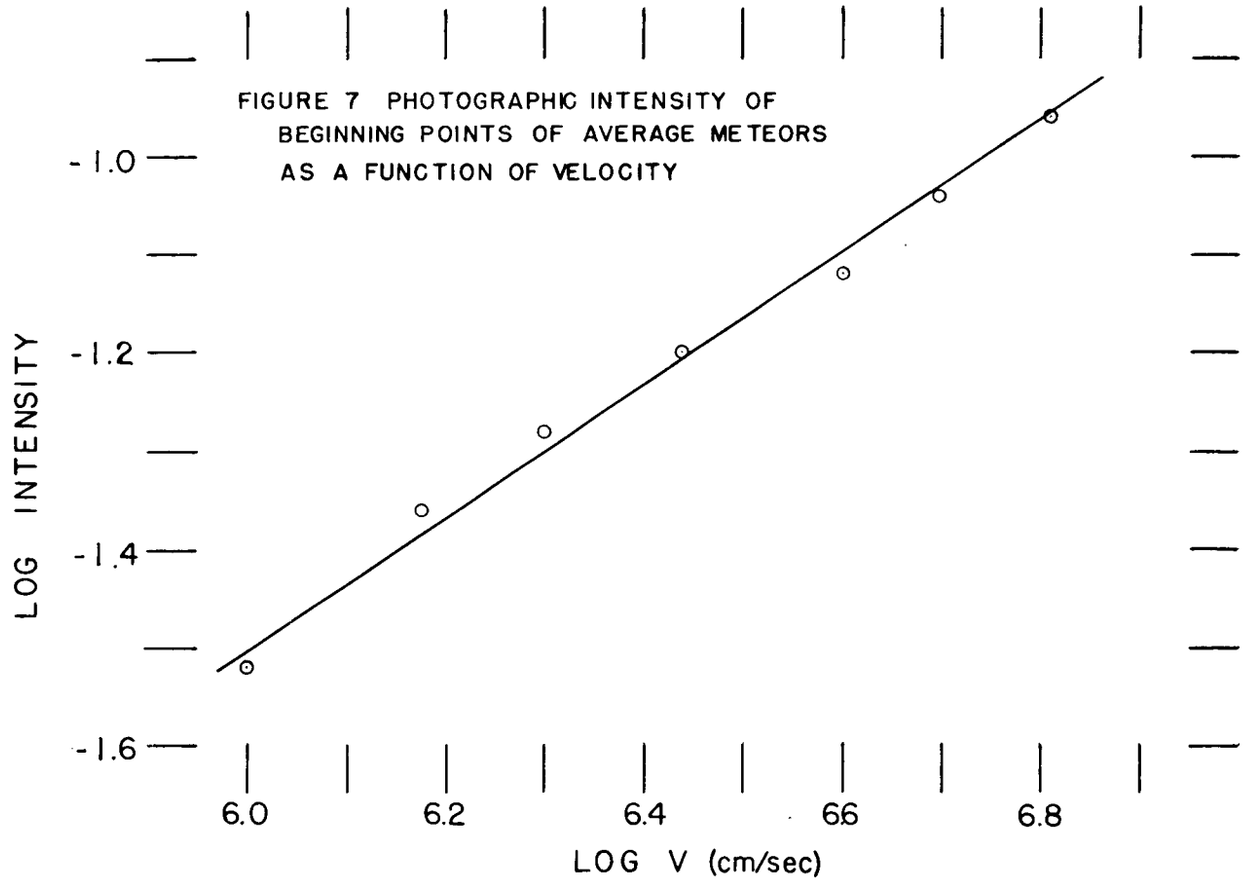

FIGURE 7 PHOTOGRAPHIC INTENSITY OF BEGINNING POINTS OF AVERAGE METEORS AS A FUNCTION OF VELOCITY

Table 19

Derivation of Photographic Intensities of Beginning Points of Faint Meteors

Velocity	10	15	20	30	40	50	65
log ρ	-7.50	-8.00	-8.35	-8.85	-9.20	-9.47	-9.79
H	77.5	84.5	89.5	96.5	102.0	106.5	112.0
h	76.0	83.0	88.0	95.0	100.5	105.0	110.5
R	80.8	88.3	93.6	101.1	106.9	111.7	117.5
m_p	10.75	11.00	11.20	11.50	11.65	11.75	11.85
M_p'	3.3	3.1	3.1	3.0	2.9	2.8	2.7
M_p	3.8	3.4	3.2	3.0	2.8	2.6	2.4
log I	-1.52	-1.36	-1.28	-1.20	-1.12	-1.04	-0.96

It is difficult to assess the accuracy of the result because we cannot be certain of the value of assumptions (a) and (b).

Summarizing some of our immediate results for the normal meteors studied here, we have

$$\rho \approx v^{-2.8}_{0.1 \pm \mu}$$

$$m \approx v^{0.7}$$

and

$$I \approx v^{\quad}.$$

We expect:

$$I \approx m^{2/3} \rho v^{\mu+\nu} \qquad (80)$$

or

$$v^{0.7} \approx v^{2/3}\,(0.1-\mu)\,v^{-2.8}\,v^{\mu+\nu}. \qquad (81)$$

Equating exponents, we arrive at:

$$\frac{1}{3}\mu + \nu = 3.4. \qquad (82)$$

If we assume the values of the standard meteor theory, $\mu = \nu = 3$, a discrepancy of about one half of a power of v exists between our results and those predicted. On the other hand, Öpik's original statement that $\tau = \tau_0 v$, which leads to $\mu = 3$, was intended to apply only to bright meteors. He predicted that for smaller bodies, τ would be independent of velocity. And indeed, Jacchia finds that for Super-Schmidt meteors, some improvement in the computed atmospheric densities results when this assumption of constant τ is employed. Our result would tend to confirm this. We have,

$$\text{if } \mu = 3, \quad \nu = 2.4$$

and

$$\text{if } \mu = 2, \quad \nu = 2.7,$$

a value which is more compatible with the assumed value of $\nu = 3$.

On the other hand, we might also explain the deviation of equation (82) from the predicted value by a change in ν. The argument in favor of this will be presented in the next chapter.

There can be some question concerning the significance of this general result. The assumptions used are reasonable and the power-law approximations are fair. However, until a more rigorous solution is performed, with a larger number of meteors, this should be accepted as a preliminary result. We believe, though, that the preceding analysis has shown the desirability of repeating the work on a more extensive scale.

CHAPTER IV

THE METEOR WAKE

A. Some Distinguishing Characteristics of Wakes and Trains

The most striking characteristic of the first Super-Schmidt meteor photographs was the frequent presence of a considerable amount of luminosity in the shutter breaks of the trails. The frontispiece shows an example of this so-called wake. Some such effect had been seen on a few photographs obtained earlier with smaller cameras (Millman and Hoffleit, 1937) but in general these cameras were too slow and the breaks too short for this phenomenon to be easily apparent. In addition, the shutters of these earlier cameras were placed in front of the objective and did not give as sharp a cut-off in the breaks as do the focal plane shutters of the Schmidts. Thus it is more difficult to recognize extraneous luminosity in these somewhat blurred breaks.

We have, in our definition and in our thinking, distinguished between the phenomena of wake and train. We have postulated that luminosity in the wake results from small particles, detached from the meteoroid proper, which decelerate with respect to the meteor and show a luminosity behind the meteor. These particles will still have a velocity comparable to that of the meteor. The train is supposed to result from recombinations of nearly stationary

atmospheric ions and atoms after the meteor has passed. The hypothesis that two separate phenomena may cause a luminosity in the breaks requires justification. Any simple inspection of the trail cannot distinguish between the two, and there appears to be no way at present by which we can show, for certain, that the wake is distinct from the train phenomena. However, the present data give us several facts which makes such a distinction entirely plausible.

First, let us assume that the intensity in the breaks is due to train, and then ask how the observed characteristics of this intensity compare with the known characteristics of a train. We know (Liller and Whipple, 1954), for example, that trains show considerable more light in the red than do meteors and we would therefore expect enhancement of the intensity in the break on panchromatic film. As yet we do not have an example of the same meteor photographed on different emulsions but this test should be kept in mind for the future. However, the complete lack of success of train photography with blue emulsions and the existence of strong wake on the same emulsions are in themselves good evidence for the belief that the two phenomena are separate.

Some information is also available on the decay time of meteor trains. Liller and Whipple assumed an arbitrary luminosity decay of the form $I = I_o/(1+ Kt)^2$ to fit the observations of meteor trains. The values of decay constant, K, depended on height and ranged in value from 0.3 to 3.0 secs^{-1}. Without concerning ourselves with an exact analysis, a visual inspection of any trail shows that the intensity of the wake has decreased by at least a factor of 2 over a distance of a dash length (1/240 sec). This order-of-magnitude calculation yields a K of 100 secs^{-1}, a value quite out of line with those for train decay. Faults can be found, however, with the above comparison. If, for example, the decay constant itself is a function of time, the comparison is not valid. Liller and Whipple derived their result from the luminosity occurring several seconds after the passage of the meteor, and our data relate to a period of time only several hundredths of a second after the meteor. Perhaps there is no reason to expect the decay factor to be constant over this range. Furthermore, the form of the decay equation may not be at all correct.

A comparison of the statistics of trains and wakes offers a more conclusive method of distinguishing between the two. We have noted (Table 13) that the existence of wake is primarily a low-velocity meteor phenomenon. Trains,

on the other hand, are distinctly associated with high-velocity meteors. Visual observers (Olivier, 1925; Norton, 1946) commonly characterize the Leonid, Orionid, Perseid and other high-velocity meteor showers as train-producing. This writer, on the basis of several years of visual observations, concurs.

The average velocity of 50 meteors in the Harvard program for which trains have been successfully photographed is 59 km/sec. Of these meteors, 40 have been reduced by the approximate method, 9 were treated by precise means and one was identified visually as a Perseid meteor for which we have assumed a velocity of 60 km/sec. We wish to thank Mr. Robert F. Hughes for a considerable portion of the approximate reductions and for supplying these data prior to publication.

Table 20 gives the velocity distributions and the corresponding distribution that would be expected if: (a) meteors produced trains independent of their velocity and (b) the distribution of meteor velocities is that given by Column (a) of Table 12 in Chapter II. The disparity is striking, between the numbers expected and those observed and cannot be explained in terms of observational selection. Although the Harvard observers in New Mexico were cognizant of the older observations concerning trains, there was a period when they thought the majority of trains they

observed visually were associated with meteors of low (apparent) velocity. However, the effort to verify this visual observation by photography failed.

Table 20

Distribution of Velocities Among Train-Producing Meteors

v (km/sec)	Observed Number	Expected Number (see text)
10-20	0	15.1
20-30	3	11.4
30-40	5	10.5
40-50	2	3.2
50-60	5	2.4
> 60	35	7.4
Total	50	50.0

Our aim has been to justify our distinguishing between wake and train, and the velocity criterion is sufficient to do so. But at the same time we may note that it is not only velocity that governs train occurrences. The observations of Trowbridge (1907), Liller (1954), and Whipple (1953) agree as to the fact that the maxima of meteor trains lie in the vicinity of 85 to 90 kilometers altitude. This region is more accessible for meteors of moderate speed (~30 km/sec) than for very fast meteors. Consequently, if slower meteors do produce trains, we would anticipate a larger number, if not a preponderance, of such

meteors among the train data.

The final point in favor of the theory that small particles cause the wake phenomena rests on Jacchia's (1955) interpretation of the anomalous behavior of faint meteors. If fragmentation does occur, we must expect a wake. The amount and the character of the wake will depend on the amount of fragmentation, the size of the fragmented particles and the known circumstances of the meteor itself (velocity, height, and trajectory). The remainder of this chapter will present a quantitative treatment of this problem.

B. Theory of the Meteor Wake

We will assume that at some time, $t = 0$, a small particle, of mass m_o, is separated from the meteoroid. We will further assume that the parent body does not shield the fragment from collision with the air molecules and that the same meteor theory may be applied to meteoroid and to wake particle. The problem will be simplified without any appreciable loss of accuracy if we suppose that the meteoroid does not decelerate during the several breaks over which we will study the fragment. We can now derive the equations giving the intensity of the wake as a function of distance behind the meteor.

The drag equation has been given as:

$$\frac{dv}{dt} = - \Gamma A \sigma_m^{-2/3} \rho_m^{-1/3} v^2 = - K_1 \rho_m^{-1/3} v^2. \qquad (83)$$

Introducing equation (14), relating the mass and velocity we find:

$$\frac{dv}{dt} = - K_1 \rho m_o^{-1/3} e^{\frac{\sigma}{6}(v_o^2 - v^2)} v^2. \qquad (84)$$

Substituting into equation (84) the relationship,

$$dt = \frac{ds}{v}, \qquad (85)$$

we find

$$\rho ds = - \frac{m_o^{1/3} e^{-\frac{\sigma}{6}(v_o^2 - v^2)}}{K_1 v} dv. \qquad (86)$$

By choosing a suitable scale height, β, we may describe the atmospheric density in a region of several kilometers by the exponential law:

$$\rho = P e^{-H/\beta}. \qquad (87)$$

The height of the meteor at any time, H, is given by $H = H_o + (s_o - s) \cos Z_R$ where Z_R is the zenith distance of the apparent radiant. We will choose our boundary conditions that at $t = t_o$, $s = 0$. All subscript zeros refer to conditions at the time the fragment separates from the meteor. Then:

$$e^{\frac{s \cos Z_R}{\beta}} ds = \left(- \frac{m_o^{1/3}}{K_1 P e^{-H_o/\beta}} \right) \frac{e^{- \frac{\sigma}{6}(v_o^2 - v^2)}}{v} dv. \qquad (88)$$

Replacing $P e^{-H_o/\beta}$ by ρ_o and integrating from 0 to s and from v_o to v we have:

$$\int_o^s de^{\frac{s \cos Z_R}{\beta}} ds = \int_v^{v_o} \left(\frac{m_o^{1/3}}{K_1 \rho_o} e^{- \frac{\sigma}{6} v_o^2} \right) \frac{e^{\frac{\sigma}{6} v^2}}{v} dv. \qquad (89)$$

In terms of a new auxiliary quantity,

$$u = \frac{\sigma}{6} v^2, \qquad (90)$$

the right hand side reduces to the difference of two exponential integrals and we obtain:

$$\left(e^{\frac{s \cos Z_R}{\beta}} - 1 \right) = \frac{E_1(u_o) - E_1(u)}{\frac{2 \beta K_1 \rho_o e^{\frac{\sigma}{6} v_o^2}}{m_o^{1/3} \cos Z_R}}, \qquad (91)$$

or

$$s = \frac{\beta}{\cos Z_R} \ln \left(\frac{E_1(u_o) - E_1(u)}{K_2} + 1 \right), \qquad (92)$$

where

$$K_2 = \frac{2 K_1 \beta \rho_o e^{\frac{\sigma}{6} v_o^2}}{m_o^{1/3} \cos Z_R}. \qquad (93)$$

The W.P.A. Tables (1940) of the exponential integrals with arguments to four places (0.000 - 9.999) were used for solutions of this equation.

Having chosen values for m_o, H_o, v_o and cos Z_R, we computed values of s for various values of v. In general, about 20 such computations were made, representing a range in v of $v_o \geq v \geq v_o - 10$ km/sec. The time elapsed since fragmentation is obtained by quadrature from the tabular relationship v versus s_w (or $\frac{1}{v}$ versus s_w) where s_w represents the distance travelled by the wake particle since fragmentation. Using this and the assumption that the meteor itself travels at constant velocity v_o, we find the lag of the wake particle, behind the meteoroid, to be

$$\Delta s = s - s_w = v_o\, t - s_w. \qquad (94)$$

Since this lag is known as a function of v, we may use the intensity equation to find the luminosity due to the wake particle as a function of the lag, Δs; that is, we may determine the intensity arising from a particle at some given distance behind the meteoroid:

$$I \text{ per particle} = \frac{\tau_o \Lambda A \delta^{-2/3} m^{2/3} \rho v^6}{4\zeta}. \qquad (95)$$

Furthermore, since we know the velocity of this particle and, by assumption, the mass of the particle at the time of fragmentation when its velocity was v_o, we may employ equation (14) to determine the mass of the particle

at the time it decelerates to a velocity v. Substituting this value of m in equation (95), we obtain:

$$\text{I per particle} = \frac{\tau_0}{4\zeta} \Lambda A^{6} m_0^{-2/3} \rho v^{6} e^{-\frac{\alpha}{3}(v_0^2 - v^2)}. \quad (96)$$

Suppose for the moment that the meteor is at rest and is a source of wake particles that accelerate away from the meteor. At the time of fragmentation, the wake particles have the same velocity as the meteor, i.e., zero velocity in the present frame of reference. Assume that fragmentations take place at a constant rate $\dot{m}_p = \left(\frac{dm}{dt}\right)_p$, and that this process has continued for a length of time sufficient to allow the first particles to have accelerated to some given velocity, say 10 km/sec. Then the current of particles is in a steady state for a distance equal to the space required for a particle to reach this velocity, and a continuity condition exists in this region. In particular, the numerical linear density of particles is given by the equation,

$$\mu\left(\frac{\text{particles}}{\text{cm}}\right) = \frac{\dot{m}_p}{m_0 v'} \quad (97)$$

where v' is the velocity of the wake particle with respect to the meteor at rest. Reverting to the usual frame of reference, we have:

$$\mu = \frac{\dot{m}_p}{(v_0 - v) m_0}. \quad (98)$$

at the time it decelerates to a velocity v. Substituting this value of m in equation (95), we obtain:

$$\text{I per particle} = \frac{\tau_0}{\mu\zeta} \Lambda A^{-2/3} m_0^{2/3} \rho v^6 e^{-\frac{\alpha}{3}(v_0^2 - v^2)}. \quad (96)$$

Suppose for the moment that the meteor is at rest and is a source of wake particles that accelerate away from the meteor. At the time of fragmentation, the wake particles have the same velocity as the meteor, i.e., zero velocity in the present frame of reference. Assume that fragmentations take place at a constant rate $\dot{m}_p = \left(\frac{dm}{dt}\right)_p$, and that this process has continued for a length of time sufficient to allow the first particles to have accelerated to some given velocity, say 10 km/sec. Then the current of particles is in a steady state for a distance equal to the space required for a particle to reach this velocity, and a continuity condition exists in this region. In particular, the numerical linear density of particles is given by the equation,

$$\mu\left(\frac{\text{particles}}{dm}\right) = \frac{\dot{m}_p}{m_0 v'} \quad (97)$$

where v' is the velocity of the wake particle with respect to the meteor at rest. Reverting to the usual frame of reference, we have:

$$\mu = \frac{\dot{m}_p}{(v_0 - v) m_0}. \quad (98)$$

Multiplying equation (96) by equation (98), we obtain a quantity, designated by $\mathcal{L}$, which we will call the linear intensity. This is the energy per second emitted by a unit length of the stream of wake material. We have then:

$$\mathcal{L} = \frac{\tau_0}{2} \frac{K_1}{\sigma} \dot{m}_p \, m_0^{-1/3} \rho v^6 \frac{e^{-\frac{\sigma}{3}(v_0^2 - v^2)}}{(v_0 - v)}, \quad (99)$$

where we have also multiplied numerator and denominator by Γ in order to transform the constants into the measured quantities, K_1 and σ.

It will be noted that equations (92) and (94), relating the lag and velocity, refer to a particle that has been fragmented at some given height, H_0, and the intensity that we derive is the intensity of this particular fragment at each point in its lifetime as it retards with respect to the meteoroid. It is this intensity which we have integrated in order to obtain the expected distribution of light in the wake, whereas actually the wake intensity at any given time is due to particles that have left the meteoroid at different times and, therefore, with a different initial condition on H_0. Our computations will be meaningful only if the conditions of the problem are such that those particles contributing light to the portion of the wake near the dash are released from the meteor at nearly the

same height as those contributing light far from the dash. If the meteor velocity is low, the particle size small and the zenith distance of the radiant large, this condition will be best fulfilled. We will concern ourselves further with this error at a later time.

For the convenience of the reader, we shall list the assumptions made up to this point.

(a) There is no appreciable deceleration of the meteoroid during the lifetime of a fragment.

(b) All fragments are initially the same size and shape.

(c) The wake particles fragment from the surface at a constant rate for at least a period of time equal to the lifetime of one particle.

(d) Each wake particle reacts with the atmosphere in the same fashion as a non-fragmenting meteor.

The assumption that we know the values of certain physical constants is implicit in (d). But the fact is, we do not. Our values of σ, derived from meteors, are neither constant nor reasonable. Also, the observed value of the density of the meteoroid, δ_m --- and thus K_1 --- may not be the same for parent body and fragment. For example, if the meteor is a hollow matrix of needles and each needle is a fragment, both the density and shape factor would differ from fragment to meteoroid. In the case of σ, we will employ the lowest value observed for

any meteor, 10^{-12} $(\frac{sec}{cm})^2$, and assume that this value is representative of a meteor which loses all of its material by evaporations. For K_1, we will use Jacchia's (1949) assumed value of 0.76 (cgs). Although an error in our choice of this constant will affect our fragment masses considerably, the results will remain self-consistent since the same factor, $K_1 m_o^{-1/3}$, appears in both of our final equations (92 and 99).

C. Observational Problems of the Meteor Wake-- A Study of a Particular Case

One meteor trail has been treated in considerable detail by the method given above. The procedure and results of this investigation are of general interest and will guide us in a following study of the expected distribution of wake among meteors of different velocity classed.

The meteor chosen for study is No. 3567, the one reproduced in enlargement in the frontispiece. It has been reduced under the direction of Dr. Jacchia who has kindly made available the results of the measurements and photometry. Some of this information is outlined in Table 21.

Table 21

General Information Relating to Meteor No. 3567

Film No.	ST 945
Date	Aug. 15, 1952
H(n = 1)*	100 km
H(n = 28)*	91 km
H(n = 38)*	88 km
v_∞	26.8 km/sec
v(n = 28)	26.6 km/sec
cos Z_R	.717
m_∞	.051 grams
log σ_{obs}	-10.9
No. of dashes, N	40

*(n refers to the dash number, the first visible dash being designated as number 1).

A low-velocity meteor was chosen to eliminate any effect of train. The analysis is based on the assumption that the entire luminosity in the breaks is due to the small particle ablation.

The curved film of the Super-Schmidt has been copied on a flat glass plate for measurements by Jacchia. The positive was used to make an enlarged (4x) negative of the meteor trail and its environs. This plate was traced along the meteor trail on a Baird densitometer, operated

with a slit width of about 1/50 of a dash length. With this densitometer, drift in the tracing can be severe if the intensity of light falling on the photocell is below a certain level. The use of the enlargement permitted the use of a relatively narrow slit without forcing the instrument to operate in this low sensitivity range. Furthermore, since our interest is primarily in the wake, the use of a negative rather than a positive print eliminates any possibility of drift being important in the breaks. The relatively slow rate of change of density in the dash makes the drift problem negligible in those regions. The diffusion resulting from the finite slit-width has been neglected in the calibration procedure.

The interpretation of such tracings is not a standard photometric problem. In the tracing of a spectrum, for example, the length of slit is not an important factor, for the density profile along the slit is essentially flat. In the case of the meteor, the profile is nearly bell-shaped and the densitometer can record only some average density over the length of the slit. If the shape of the profile and the shape of the characteristic curve are known, one can indeed determine the original intensity that produced the image but the procedure would be time-consuming. And in any case, we have no first-hand knowledge of the characteristic curve. Star images can supply this, but we

have preferred to by-pass this step in favor of a more direct method. The usual method (Jacchia, 1949) of meteor photometry gives us an intensity scale that applies directly to the meteor images. We can associate a densitometer scale reading (which for the reason just given should not be called a density) with the photometric magnitude for each dash. For meteor No. 3567 a range of about 3 magnitudes exists between the extremes in intensity.

Tracings were made with several different slit lengths, ranging from a length that slightly exceeded the breadth of the brightest image to a length of half this amount. In each case a good linear relationship between scale reading and observed magnitude was obtained. The shortest width was finally employed since it gave the greatest contrast in scale readings.

Since the maxima of intensity of the dashes on this meteor do not exhibit flat tops, there is some question concerning what scale reading should be attributed to the observed magnitude. In comparing meteor dashes with trailed star images, as is done in visual photometry, one would expect the eye to judge on the basis of an extended image and thus derive some integrated magnitude that was less than that of the maximum. Since photometry is carried out with star images which are trailed a distance equal to

the length of a meteor dash, we decided to accept the value of the scale reading at the point where the rising and falling branches of the scale-reading curve were separated by a distance of 1/2 dash length. This is roughly comparable to assuming that the individual responsible for the photometry chooses for comparison a star image whose density would be equal to the density of the meteor if the intensity causing the meteor image had been smoothed out evenly over one dash length. We have not looked for an exact criterion here, we can only make an intelligent approximation. The final results do not depend critically on our choice in this matter.

Figure 8 gives the results of this calibration. The magnitudes are absolute photographic. The curve is based on 40 points representing photometric estimates and densitometer readings on as many dashes. Jacchia considers these magnitudes to be accurate to within $0^m.1$ or $0^m.2$ in regions of moderate density.* The individual points are compatible with this estimated figure. Depending on individual preference for results obtained by an experienced visual observer or for those obtained from an

---

* Jacchia has employed no correction for any reciprocity law failure that may exist between meteor exposures ($\sim 10^{-3}$ seconds) and trailed star images ($\sim$1 second). We have followed this procedure here although we believe the need for such a correction may well exist. The question must be considered open until more information on the emulsion becomes available.

FIGURE 8 CALIBRATION CURVE FOR METEOR NO. 3567

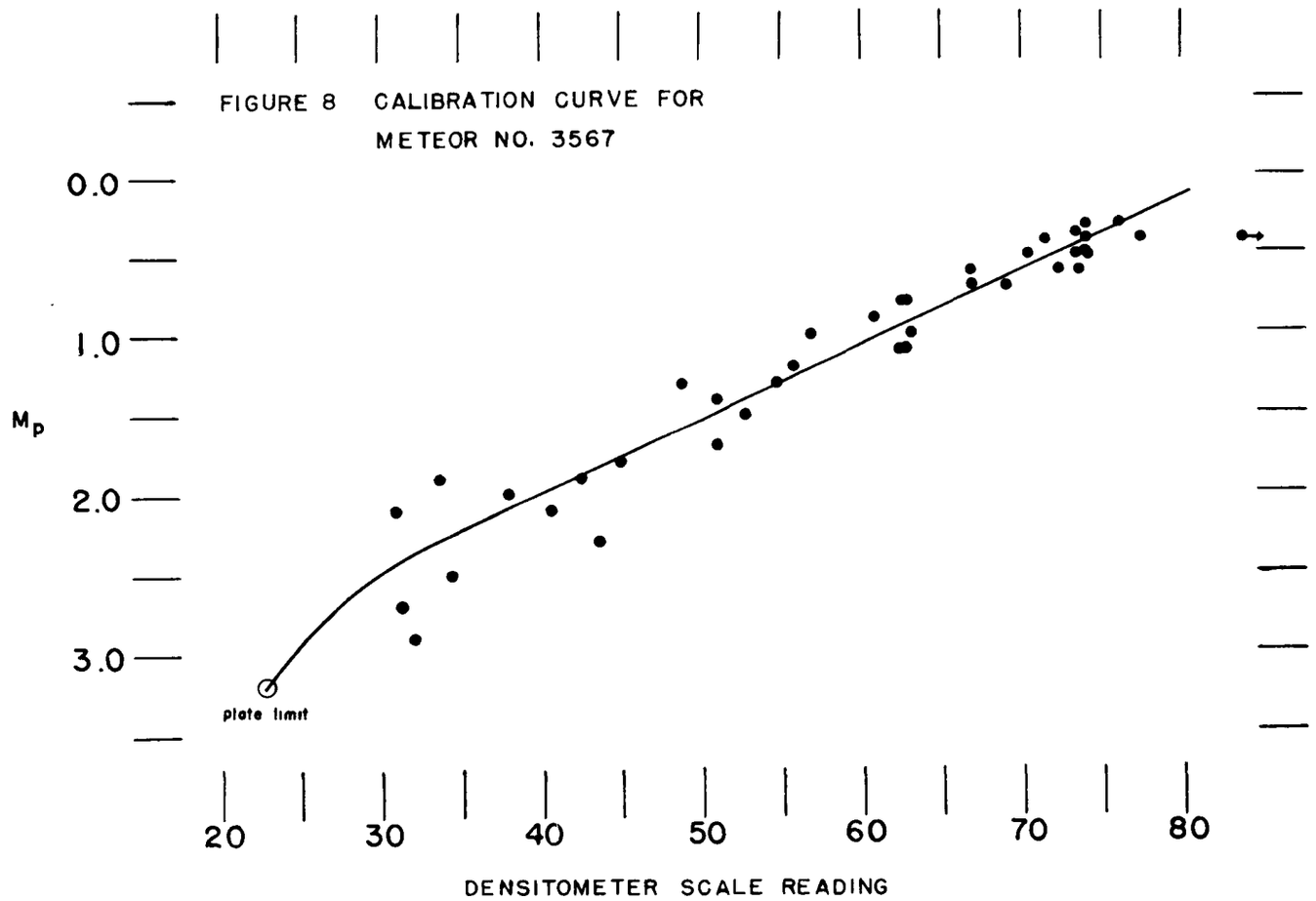

accurate densitometer necessarily used ineptly, one can justify the accuracy of the other.

For the study of the wake, six dashes (n = 25 to 31) were chosen. The meteor shows strong wake in this region. These breaks do not differ markedly from one another and the tracings indicate that no stars of appreciable brightness are superimposed on the trail. However, we decided to average the scale readings, rather than intensities, for these breaks in order to diminish the importance of any fainter star images that might be present. Before the averaging process could be carried out, it was necessary to determine some zero point in each dash tracing. The point of maximum light appeared to be the obvious choice of a well defined position on each break. It was found, though, that the distances between maxima did not change monotonically. It was rather surprising to find, then, that the points of minimum light were separated by a nearly constant distance and offered a far better choice of a zero point.

Scale readings were recorded for 26 points, separated by equal intervals, in each of the six break and dash cycles. These may be found in Table 22, reproduced here in place of the actual tracings. The homogeneity among the six breaks will be noted. The last column is the average density profile. It is this observed average of the six shutter cycles that we will attempt to reproduce by computations. Curve A, Figure 9, shows in graphical form

Table 22

Values of Scale Readings for Selected Positions on Six Shutter Cycles of Meteor No. 3567

Break No.	26	27	28	29	30	31	(Average)
Fraction							
0	35.0	38.7	37.0	37.2	37.3	35.3	36.75
1	35.2	38.9	38.0	37.6	36.9	35.6	37.03
2	36.8	39.6	39.2	38.7	37.3	36.7	38.05
3	38.1	40.4	40.1	40.6	38.8	38.2	39.37
4	40.0	41.7	41.5	42.8	41.0	40.3	41.22
5	42.0	43.1	43.2	44.9	43.5	42.8	43.25
6	44.2	45.0	45.5	46.9	47.1	45.0	45.62
7	47.0	47.6	48.7	49.9	50.0	48.4	48.60
8	49.8	50.2	51.2	54.3	53.1	50.7	51.55
9	54.0	53.9	55.2	58.2	57.0	53.0	55.22
10	58.6	58.7	59.2	62.9	61.3	56.8	59.58
11	63.3	63.3	64.1	66.4	65.1	61.0	63.87
12	68.0	68.6	68.0	70.7	68.6	65.0	68.15
13	72.3	72.8	71.4	73.3	71.8	70.0	71.93
14	74.8	75.2	74.1	74.9	73.8	73.3	74.35
15	76.0	76.1	75.1	75.3	75.1	76.3	75.65
16	76.1	76.1	75.5	74.8	75.9	78.4	76.13
17	75.3	74.8	75.0	73.7	75.7	78.3	75.47
18	73.0	72.4	73.5	71.8	75.0	76.6	73.72
19	68.8	68.3	69.9	69.0	71.6	73.1	70.12
20	63.0	61.8	64.3	66.3	66.0	68.5	64.98
21	55.0	54.7	59.0	61.0	60.0	61.7	58.57
22	46.9	47.5	53.0	55.4	52.6	53.9	51.55
23	42.3	41.7	46.8	49.3	46.4	45.2	45.28
24	39.4	38.7	41.7	44.5	41.7	39.5	40.92
25	38.6	36.9	39.0	40.3	37.2	36.1	38.02
26	38.6	36.9	37.4	38.0	35.7	35.2	36.97

the densitometer readings as a function of the break-dash cycle ($\Delta n = 1$ represents one shutter cycle). The round top is characteristic of each dash and is not a result of smoothing by the averaging process. It should also be noted that the scale readings for most of the cycle lie between

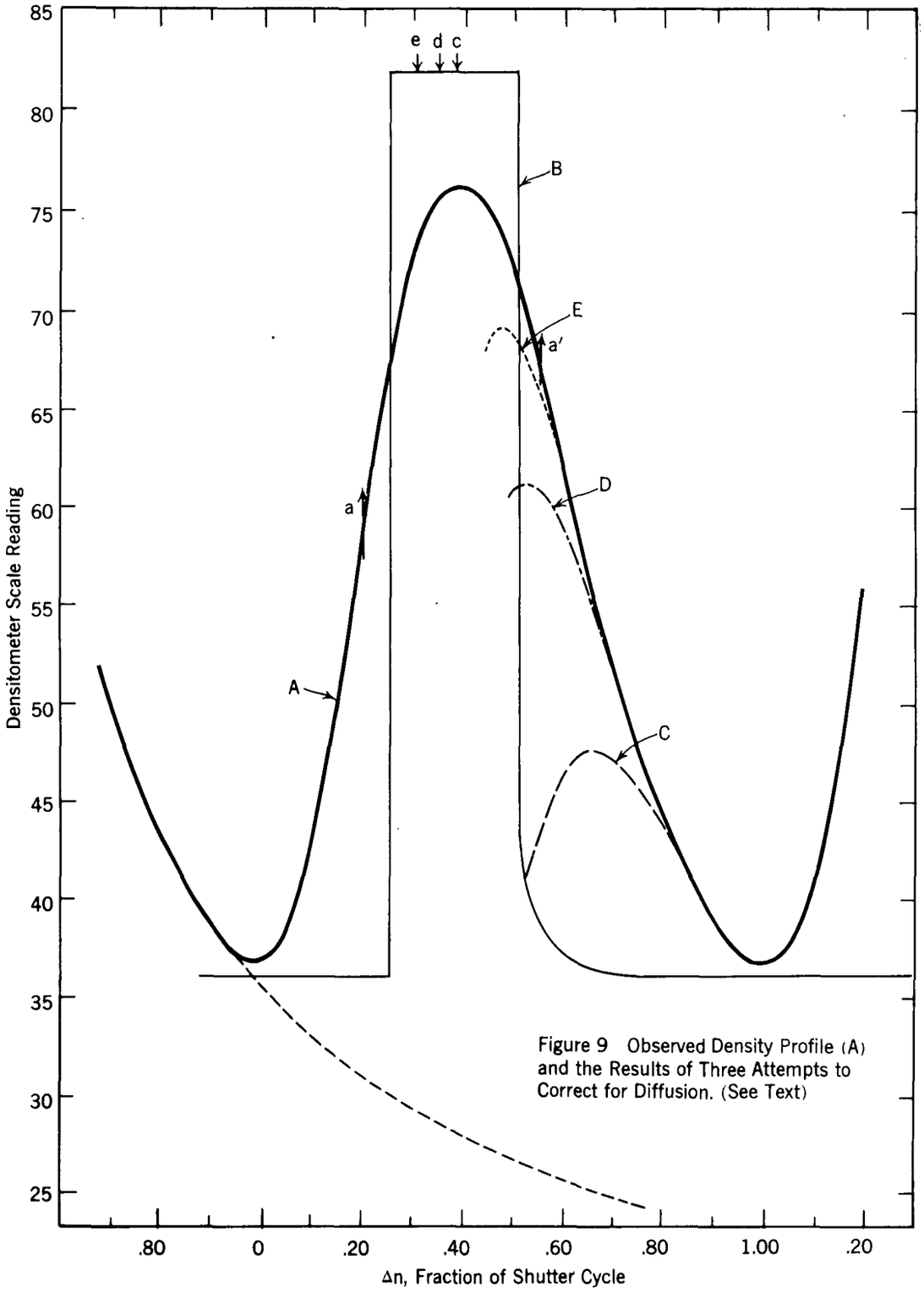

Figure 9 Observed Density Profile (A) and the Results of Three Attempts to Correct for Diffusion. (See Text)

40 and 75 where the calibration is best determined (see Figure 8). This was not a matter of pure chance. Meteor No. 3567 was selected from several dozen others for a variety of reasons. Its low velocity and assumed absence of train have been mentioned. The appearance of the strong wake, well above the photographic threshold value, is another. A stronger wake image could have been obtained by choosing a meteor in poorer projection against the plane of the sky, i.e., a meteor at a smaller distance from the radiant, but this would have intensified the problem of correcting for the photographic diffusion of the meteor image into the wake. The present example is a compromise between high density images and low diffusion.

Our general approach to the analysis of these raw data originally followed these lines:

(a) Correct, by some means, the intensity profile for photographic diffusion.

(b) Find that size of particle, fragmented from the meteor, which would cause the observed slope in the intensity-lag curve of the wake. We do not intend to insist on the validity of the assumption that particles of only one size are responsible for the wake, but our data are not sufficiently good to determine a meaningful distribution of particle sizes. Thus, the best approach seems to be an attempt to find that one size which can best

characterize the observations.

(c) In process (b), we have determined one of the desired factors, m_o, by fitting observed and computed slopes of the wake intensity curve. The other unknown, $\dot{m}_p$, in our basic equation (99) is fixed by the integrated intensity in the wake.

The question of correcting the observed profile for effects of diffusion becomes, as will be seen, the crux of the entire problem of meteor fragmentation. For the first attempt, we made the assumption that the major part of the light of a meteor was derived from the meteoroid itself and that, consequently, the wake represented only a small perturbation on the total light. If this is so, the maxima of the dash will represent the position of the meteor after it has traveled half the distance of the dash. These assumptions would predict an undiffused profile similar to that of Curve B, Figure 9. We can use the difference in intensity between the observed and undiffused curves at any point, say "a" in Figure 9, to the left of maximum light to correct the corresponding point,"a", an equal distance to the right of maximum light. As a modest refinement of this method, we have corrected the leading edge of the dash to a point determined by the wake of the next cycle. The dotted extrapolation of Curve A in Figure 9 represents our estimate of this intensity.

The resulting curve in the wake, rectified by the procedure described above, is expressed as Curve C in Figure 9. It should be clear from the description of the method of wake formation that such an intensity distribution behind the meteor is an impossibility. At the time of fragmentation, the particles have their highest velocity, greatest mass and strongest concentration along the meteor path. All of these factors act to produce a constant decrease in wake intensity with increasing distance from the meteor. Only the air density, ρ, can act to increase the luminosity and this effect is negligible for particles of short lifetime. We can, by radically changing our thinking on the wake process, construct a model to explain this light curve, but we have not found what we believe to be a reasonable model. We could, for example, assume that particles disengage themselves from the meteor, decelerate with respect to it, and then fragment into still smaller pieces. One would prefer much stronger evidence for this complicated technique before accepting it.

We can reduce the extent of the departure of the wake from a monotonic curve by assuming that the maximum light does not represent the position of the meteor at the center of the dash exposure. In this case, then, we are assuming that an appreciable fraction of the light comes from the wake - a fraction large enough to shift the center of light to an

earlier portion of the dash. If this is true, we are no longer justified in assuming the same excess of light due to diffusion for points at equal distances to the left and to the right of the chosen center. Or, in other terms, the wake is no longer a small perturbation on the total intensity and we must be concerned with the diffusion of <u>its</u> luminosity. Nevertheless, if we were to find that this effect is small (but not negligible), we might conclude that the simplified diffusion correction used up to the present would supply at least a good first approximation.

To test this, several rectified wake curves were computed on the assumption that the center of the meteor would be found at some point to the right of maximum light. Centers were chosen at the points marked d and e. The resulting rectified wake curves are given as Curves D and E, Figure 9. Only when the maximum intensity of the wake approaches that of the meteor do we find a curve that might represent the intensity of fragmented particles. We must approach the diffusion problem in another way; we cannot think of the wake as producing an amount of light very small compared to that of the meteoroid.

The general diffusion equation,

$$F(x) = \int_{-\infty}^{\infty} f(x-\epsilon)\, g(\epsilon)\, d\epsilon \,, \qquad (100)$$

relates an observed function, F(x), with an (undiffused) function, f(x) through an error function, g(ϵ) which in this case will be a measure of the degree of photographic image spreading - as caused by aberrations, turbidity of emulsion and seeing - and of the smoothing effect of the finite width of the densitometer slit. To a first approximation, the intensity curve derived from a tracing of a star image may be used as an error function. Several stars near the meteor trail on film ST 945 were traced with the same slit employed for the meteor. These images show a certain amount of trailing but this does not affect the results if the tracing is made with the slit lying parallel to the long axis of the star image.

Because of the characteristic of the reciprocity law failure for the X-Ray emulsion, we cannot use the same calibration curve for meteors and for stars. The Eastman-Kodak Company has supplied us with the reciprocity failure curves for densities of 0.6 and 1.0. Assuming these points lie on the straight line portion of the H-D curve, we can write

$$D = \gamma\, (\log It - \log i) \qquad (101)$$

and solve for the inertia point and the slope at various exposure times. The results for the two cases, representing approximately the exposure times for meteors (~0.001 sec) and for tracked stars (3 minutes) are found in Table 23.

Table 23

Effect of Reciprocity Law Failure on the Characteristic Curve of X-Ray Emulsion

Exposure time (secs)	$10^{2.5}$	$10^{0.5}$
Density	log It (MC-sec)	
0.6	-1.36	-1.75
1.0	-1.00	-1.44
γ	1.1	1.3
log i	-1.90	-2.22

To interpret the density readings obtained from the star tracings, we shall use the ratio of $\frac{\gamma \text{ star}}{\gamma \text{ meteor}}$ to correct our calibration curve, Figure 8. Since we wish to normalize the star-intensity profile, we need not concern ourselves with any more nearly absolute intensity units.

The normalized profile of the star, as a function of distance measured on a scale of 1 = break-dash cycle, is given in Column 2 of Table 24. This observed curve can be quite well represented by an error function of the usual form,

$$g(\epsilon) = \frac{h}{\sqrt{\pi}} e^{-h^2 \epsilon^2}, \qquad (102)$$

if we choose the dispersion parameter to be

$$h = 0.35.$$

This computed function is given in Column 3 of Table 24 for comparison.

Table 24

Observed and Computed Intensity Profiles for Point Source Images

Distance from Image Center	Observed	Computed (h = 0.35)	Computed (h = 0.175)
0	.198	.198	.098
0.025	.178	.175	.096
0.050	.110	.121	.088
0.075	.059	.066	.076
0.100	.024	.024	.061
0.125	.015	.009	.046
0.150	.007	.002	.033
0.175	.001	.000	.022
0.200	0	0	.014
0.225	0	0	.008
0.250	0	0	.005
0.275	0	0	.002

We have stated that the star image profile is a good first approximation to the error function, in that a point-source profile should properly account for most of the diffusing elements of the image and tracing. It fails,

however, in one respect. Meteor images on the Super-Schmidts are noticeably out of focus compared to star images, because of the color differences. It has been found that one can duplicate the character of meteor images by using trailed star images that are obtained with the focal length shortened by about 25 to 100 microns. Using the known angle of the beam at the focus of this f/0.65 system, we can obtain a fair estimate of the increased dispersion resulting from improper focus. Although the camera is capable of producing star images of 15 microns, under field conditions of changing temperature and inexact focal settings, somewhat larger images should probably be expected. We have assumed them to be 20μ. A change of focus of 25μ would then almost double the image size. Such a line of reasoning has led us to adopt an error function, for the meteor images, of the same analytic form as that obtained for the star but with the diffusion modulus, $\underline{h}$, equal to half that of the star. It is difficult to estimate the error that might be expected in such an approximation. Using an out-of-focus star image might seem to be preferable to making the assumption concerning the form of the error curve. Then, however, we would need a comparison of the characteristic curves of the enlarged negatives of both the meteor photograph and the out-of-focus star photograph. In the absence of any real intensity standards on the star plate, it would be necessary to assume

that the two photographs had been treated identically in the many processes between the initial photograph and the final enlargement. The alternative assumption, as used, of the form of the error curve does not appear to be any less satisfactory. The writer feels that any estimate of h for meteors between the values of 0.10 to 0.20 could be justified. If, instead of h = 0.175, we used twice this value for the diffusion parameter, we can still find a particle size that will reproduce the observed intensity curve. In this case, the particle size is less than an order of magnitude larger than the mass we shall show to be most acceptable.

Using h = 0.175, we obtain the error function for the diffusion of the meteor intensity as given in the fourth column of Table 24. This error function is the one that will be used in the solution of equation (100).

Our second attempt to correct for diffusion was also abortive. We used a method due to Öpik and described in an unpublished manuscript by Bok and de Jonge (see also de Jonge, 1954). First we "diffuse" the observed function curve, obtaining

$$F'(x) = \int f(x-\epsilon)\, g(\epsilon)\, d\epsilon, \qquad (103)$$

and then correct the observed function to obtain the true function by the equation

$$f(x) = F(x) + \left[F(x) - F'(x)\right]. \qquad (104)$$

This is tantamount to the assumption that successive applications of the diffusion equation will yield the same change in the ordinate for any given x. Bok and de Jonge showed that more refined methods were necessary when the distribution was skew, as is ours. But more important, such a method must fail when the diffusion is not reasonably small. The application of this method to our functions resulted in some negative intensities for the "true" function. Other logical inconsistencies, related to the ratio of the intensity in the wake and in the dash, demonstrated conclusively that we had overstepped the bounds of reasonableness in attempting to apply the approximation.

Before continuing with the third attempt at correcting the diffusion, let us return a moment to our first method. We were led to that approach not only by its simplicity, but also by a preconceived notion that all meteors produce <u>most</u> of their light by atomic ablation directly from the meteoroid. The first approach has shown that at least a modest fraction of the light arises from the smaller wake particles. Our third approach, then, will start from the assumption that <u>all</u> of the meteor luminosity is produced by the wake particles. This, as it happens, is a better first approximation, and will make it easier to produce a

second approximation. The greater flexibility results from the independent determination of the diffusion function. We are no longer requiring that the data from the meteor trail alone supply all of the answers.

Let us outline the method:

(a) We first compute, by means of equation (99), the linear intensity, Q, as a function of the lag, Δs, due to particles of some given initial mass, m_o.

For convenience of explanation, we will express the lag, Δs, in terms of a fraction of the shutter cycle, n, by means of the relation

$$n = 60 \frac{\Delta s}{v_o}, \qquad (105)$$

where the figure 60 represents the number of shutter cycles per second.

(b) Our computations in (a) do not lead to a quantity that we may observe directly on a meteor photograph. In essence, (a) yields an intensity distribution as a function of distance behind the meteor; this is what we would photograph if an infinitesimally short exposure were made of the meteor. The actual exposures are not of this nature and we must

account for the "smearing" caused by the motion of the meteor during the period of time the shutter is open. As a particular example, the intensity we photograph at the point where the dash and the wake join is due to the sum of the intensity at this point and at all parts of the wake behind it that will, as a result of the meteor's motion, reach this point in space before the shutter closes again. Since the shutter remains open for 1/4 of a cycle ($\Delta n = 0.25$), we must integrate the linear intensity over this distance. This, stated analytically, is

$$I_{\Delta n = 0} = \int_{\Delta n = 0}^{\Delta n = 0.25} \mathcal{I}\, ds, \qquad (106)$$

or, for the general case,

$$I_{\Delta n} = \int_{\Delta n}^{\Delta n + 0.25} \mathcal{I}\, ds. \qquad (107)$$

These results are obtained by plotting $\mathcal{I}$ as a function of Δn and by measuring areas with a planimeter. It will be noted that the part of the cycle <u>in</u> the dash ($-0.25 < \Delta n < 0$) receives part of its contribution from the

wake in the next cycle.

(c) Using the true function obtained in (b) and the error function derived in Table 24, we apply the diffusion equation, integrating by quadrature to obtain a computed function that may be compared with the observed curve.

(d) Primarily, we are attempting to find a computed curve whose slope will match that of the observed curve in the region of the wake. However, since our first approximation calls for the entire light to arise from the wake, the comparison of (c) with the observed function should be made with the maxima of the two curves superimposed. A small relative shift between these curves could be compensated for by the addition of some light produced by the meteoroid.

(e) Let us assume that we have found the proper value of m_o to fit the slope of the computed curve to the observed curve in the region of the wake. In order to make the curves match with respect to their total intensities, we may adjust $\hat{m}_p$ in equation (99). And, of course, we will at the same time be adjusting the magnitude of the computed curve in the region of the dash.

We require that the computed curve should not contain a greater integrated intensity than does the observed curve in the region of the dash. Allowing the meteoroid to produce no light is a severe enough change in our thinking -- we cannot expect it to produce negative light.

(f) We should expect, if our reasoning and computations are correct, to find some value of m_o that satisfies the criteria of slope and intensity. Such a particle size, at a given $\dot{m}_p$, will produce the wake and part, if not all, of the intensity we see in the dash. Whatever needed intensity the particles fail to supply to the dash, we will make up with light from the meteoroid. It will then be necessary to recompute the distribution through the diffusion equation, and to add to the true intensity in the dash that which is due to the meteoroid. If this addition is small, one would expect the second approximation to be sufficient.

This, then, is the procedure we have been forced to adopt. Mathematically speaking, it is not as nice as the previous methods. We must perform the computations needed to "diffuse" the results of light curves for many different particle sizes. In the first trial we used a value of $m_o = 10^{-8}$

grams. Curve "A" of Figure 10 is the computed (undiffused) intensity curve for the wake particles, given as a function of Δn. We have adjusted the amplitude of the curve by assuming a value of $\hat{m}_p$ which equalizes the integrated intensities of this computed curve and of the observed curve, marked "C". Curve "B" is the computed curve diffused by the error function. The computed curve, in the wake, falls below the observed curve. If we force them to match by increasing $\hat{m}_p$, we will increase the total amount of light produced by the particles to a value exceeding the total light observed. Consequently we must adjust the particle size.

There might be some question as to the direction in which we choose to make this adjustment. If we consider the two extreme cases in which: (a), the meteor ablates the smallest particles possible (atoms), and (b), meteor ablates the largest particle possible (meteor breaks into two equal pieces), we see that both cases lead to zero wake-intensity. Between these two extremes, then, there must be some value of m_o which produces a maximum of wake. The familiarity with the equations, gained in the first calculation, is sufficient for us to realize that in the present case we need an increase in the size of the particles.

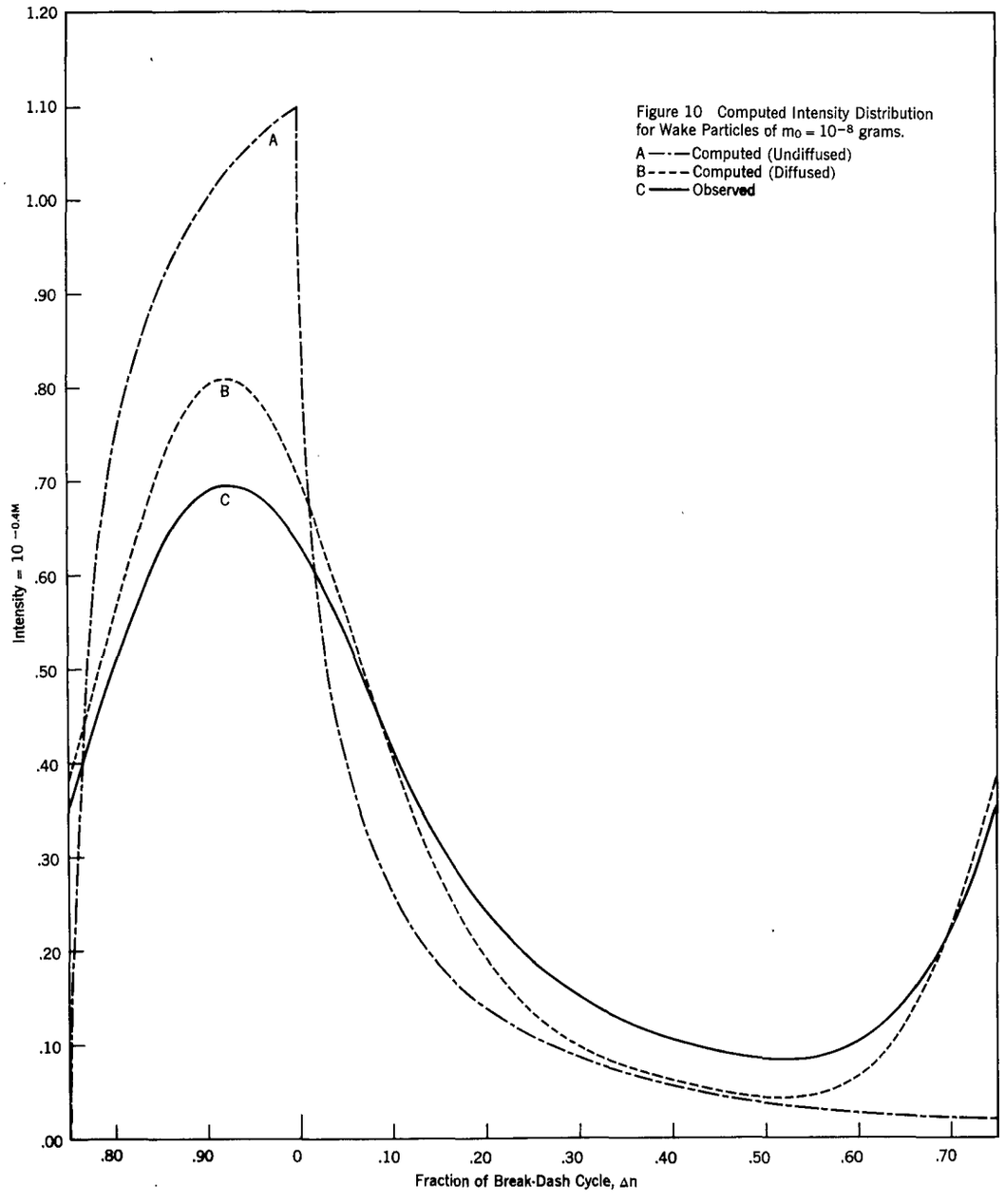

Figure 10 Computed Intensity Distribution for Wake Particles of $m_0 = 10^{-8}$ grams.

A —·—·— Computed (Undiffused)
B - - - - Computed (Diffused)
C ——— Observed

The results for $m_o = 10^{-6}$ grams, treated in the same fashion as above, are found in Figure 16. The fit of the observed and computed curves is extremely good. Note that in this case the entire luminosity can be attributed to the fragmented particles. Before discussing this result, we will present, in Figures 12 and 13, the results for still larger particles, $m_o = 10^{-5}$ grams and $m_o = 10^{-4}$ grams. In both of these cases we can obtain a satisfactory agreement with the observational curve by a proper choice of $\dot{m}_p$ and I_b, the intensity produced by the unfragmented meteoroid. It is probable that agreement could be improved somewhat for all of the last three cases ($m_o = 10^{-6}$, 10^{-5}, 10^{-4}) by a more careful selection of the parameters $\dot{m}_p$ and I_b. The nature and quality of the data make such refinements meaningless. We may consider that any one of these three results fit the observations.

The preceding analysis has supplied us with a lower limit to the particle size that may be used to describe the meteor wake. Particles smaller than 10^{-6} grams cannot reproduce the light curve of the wake without exceeding the total luminosity of the meteor. The upper limit is not as clearly defined. From the data presented so far, we might presume that particles of 10^{-3} grams or even 10^{-2} grams could satisfy all of the observed luminosity conditions. However, we will show that such particle sizes would not be consistent with the known duration of the meteor.

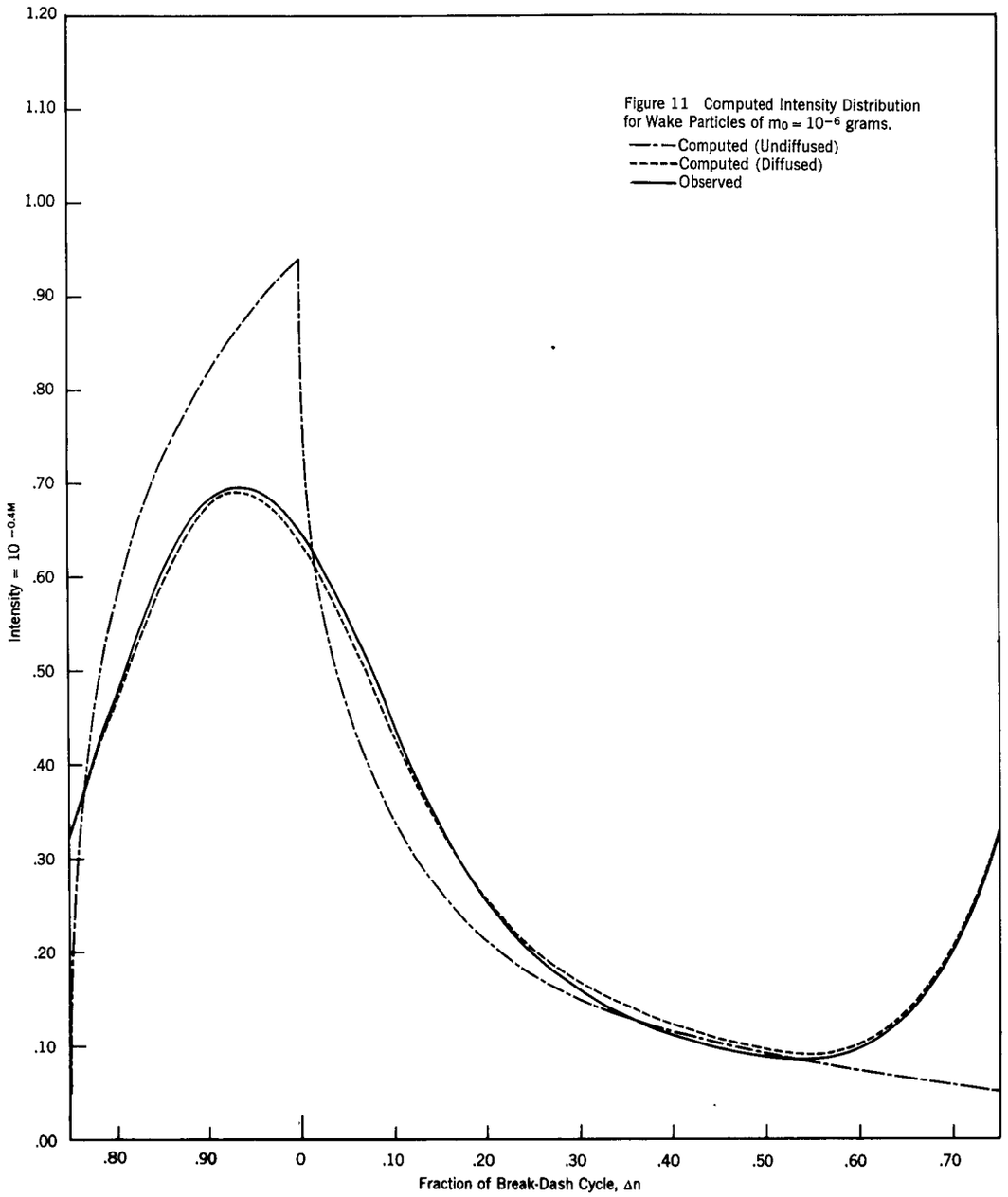

Figure 11 Computed Intensity Distribution for Wake Particles of $m_0 \approx 10^{-6}$ grams.

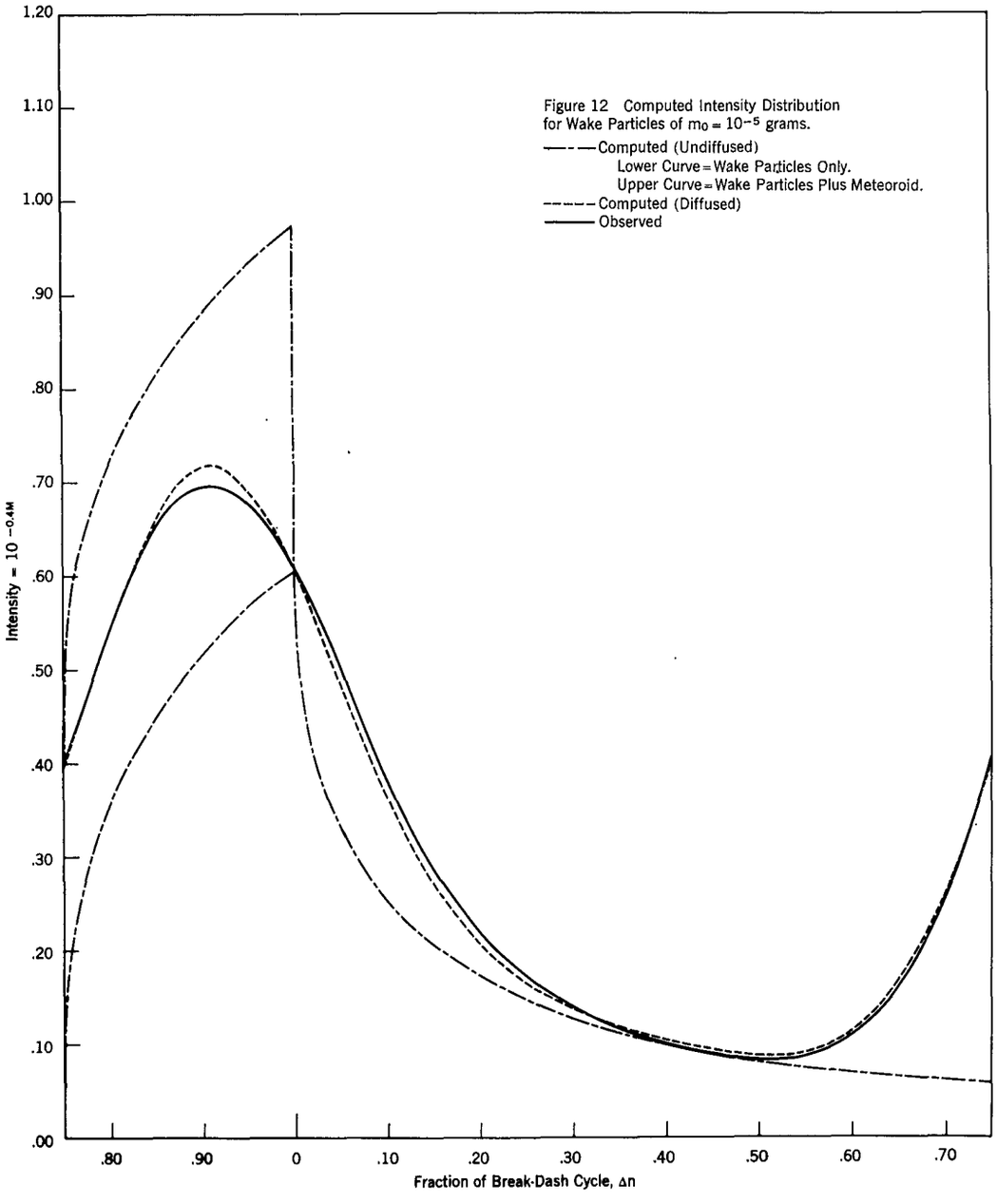
1.20
1.10
1.00
.90
.80
.70
.60
.50
.40
.30
.20
.10
.00
Intensity = 10 −0.4M
.80
.90
0
.10
.20
.30
.40
.50
.60
.70
Fraction of Break-Dash Cycle, Δn
Figure 12 Computed Intensity Distribution
for Wake Particles of m0 = 10−5 grams.
Computed (Undiffused)
Lower Curve = Wake Particles Only.
Upper Curve = Wake Particles Plus Meteoroid.
Computed (Diffused)
Observed

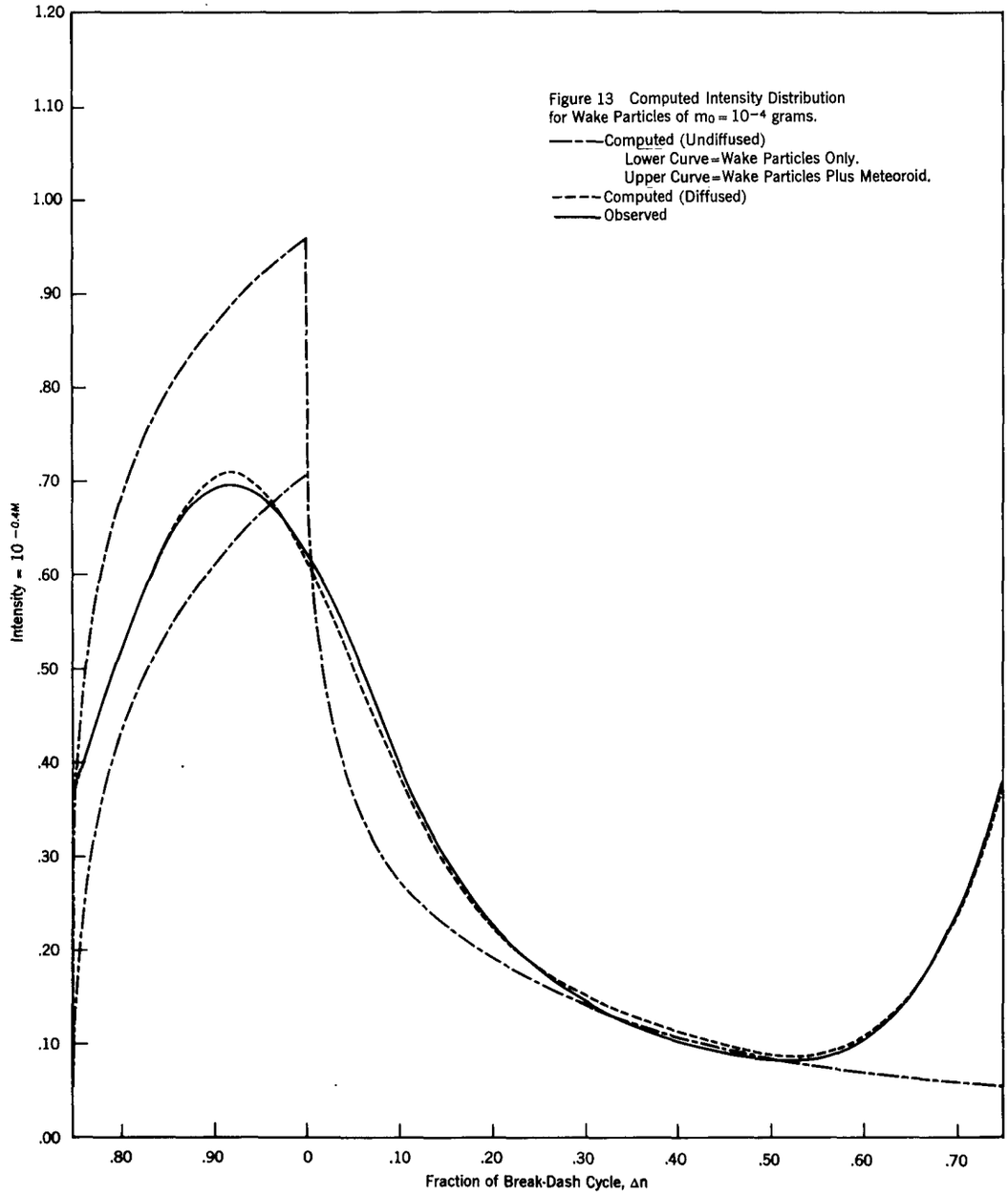
1.20
1.10
1.00
.90
.80
.70
.60
.50
.40
.30
.20
.10
.00
Intensity = 10 −0.4M
.80
.90
0
.10
.20
.30
.40
.50
.60
.70
Fraction of Break-Dash Cycle, Δn
Figure 13 Computed Intensity Distribution
for Wake Particles of m0 = 10−4 grams.
Computed (Undiffused)
Lower Curve=Wake Particles Only.
Upper Curve=Wake Particles Plus Meteoroid.
Computed (Diffused)
Observed

Depending on the mass of the wake particle, a certain amount of time is necessary for the particle to lag behind the meteoroid sufficiently to produce luminosity in the wake. Figure 14 is a plot of the number of breaks (n) after fragmentation traveled by the meteor before particles of initial size m_o lag by $\Delta n = 0.25$. The dotted section of the curve is an exponential extrapolation.

Wake becomes obvious in this meteor by the position $n = 14$. If we were to choose a particle size of $m_o = 10^{-4}$, this would require that an appreciable fragmentation should have taken place before the meteor was visible. Since most of the light of the wake particles is expended at a point in or near the dash, the meteor must be visible as soon as it fragments a sufficient amount to produce wake (unless, of course, the fragmentation occurs at heights so great that the air density is too low for any vaporization to take place). Consequently, we may set an upper limit of about 10^{-4} grams on the particle size that may be used to describe the wake. In this case, the fragments still produce a large amount of the total light produced by the meteor.

Additional information may be utilized to assist us in making a choice of the particle size that should be attributed to the wake. First, we may use the value of σ measured by Jacchia for this meteor (see Table 21) to determine a reasonable ratio of the area of the meteoroid and the total

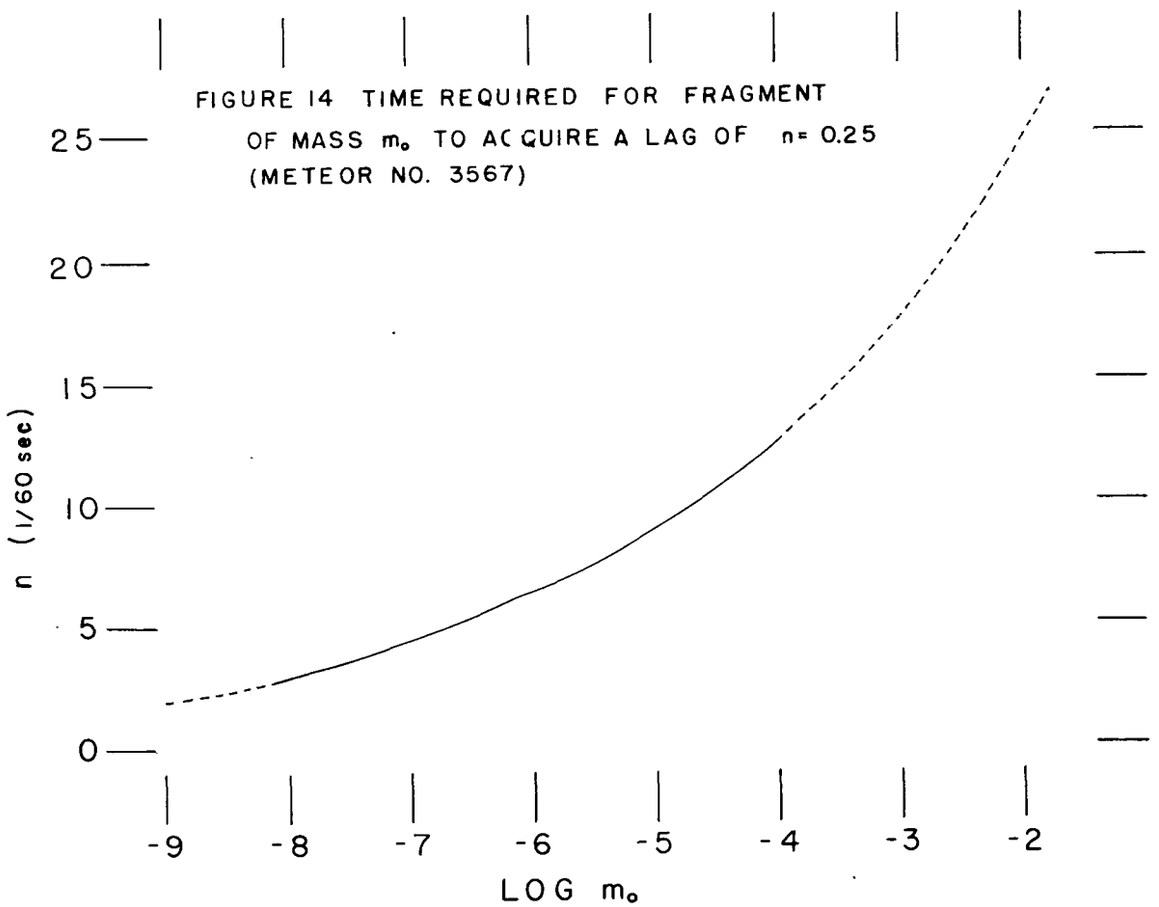

FIGURE 14 TIME REQUIRED FOR FRAGMENT OF MASS m_o TO ACQUIRE A LAG OF $n = 0.25$ (METEOR NO. 3567)

area of the wake particles. We have already derived (equation (25), Chapter I) this relationship for a meteor fragmenting in the manner we have assumed for these calculations. To acquire an estimate of the expected value of σ_{obs}, we may use the ratio of the luminosity caused by the wake particles and the meteoroid to represent the ratio of the areas of the wake particles and meteoroid,

$$\frac{A_p}{A_b} = \frac{I_p}{I_b} . \qquad (108)$$

This would be valid if all the wake particles possessed the same velocity as the meteoroid; then total intensities would be proportional to total area. Since the particles produce most of their luminosity when they are moving at velocities essentially equal to that of the meteoroid, equation (25) is a very good approximation.

We will also neglect the correction to σ_{obs} necessitated by the use of too great a mass in equation (13) (see Chapter I, page 18). We might estimate that these two effects, taken into account, would serve to increase the value of σ_{obs} by less than 25 percent.

Table 25 gives the value of σ_{obs} predicted for each of the three possible sizes of wake particles. This value is based on the assumption that the true value of σ is

Table 25

Parameters Derived from Computations Performed to Determine the Size of Wake-Producing Particles

Initial size of particle, m_o (grams)	10^{-8}	10^{-6}	10^{-5}	10^{-4}
Rate of mass loss by fragmentation, $\dot{m}_p$ (grams/sec)	.285	.369	.369	.427
Luminosity produced directly by meteoroid, I_b	(<0)	0	.253	.366
Ratio of luminosities of wake particles and meteoroid, I_p/I_b	-----	∞	3.9	2.4
Predicted value of log σ_{obs} (sec/km)^2 (to be compared with -10.9)	-----	∞	-11.3	-11.5

10^{-12} $(\frac{sec}{km})^2$, the value used in the computations. We have also summarized the other important quantities derived from the calculations. These results tend to substantiate the previous conclusions on the best particle size and, indeed, narrow down the limits of acceptability. The particle size best suited for reproducing the wake phenomena would appear to be between 10^{-6} and 10^{-5} grams. It is interesting to note that this value agrees extremely well with those deduced by Smith (1954) for meteor flare particles. Since the ballistic constants employed by Smith agree closely with ours, we may compare masses directly. His average value, for 27 determinations of 14 flares, was $5 \cdot 10^{-6}$ grams.

At the time Smith did his work, the concept of very fragile meteors of low density had not been fully developed. The only feasible explanation for flares at that time was one of molten droplets shedding from the meteoroid. If, however, meteors are of such low densities as we now believe, there appears to be no escape from the conclusion that they are a matrix of material. How else shall we form a meteor, which we know contains heavier elements, unless there exists a considerable amount of empty space in the body?

If surface melting occurred in a body of this sort, one would expect the molten material to flow into the interstices. This, coupled with the apparent pressure fracturing of the abrupt meteors (Chapter III) make it seem most likely that all meteoroids fragment solid particles from the surface.

D. <u>The Meteor Wake -- The General Case</u>

We may utilize the information obtained in the previous discussion to inspect some broader aspects of the wake phenomenon. The reader should bear in mind the various inadequacies of the data that yielded the particle size. In particular we wish to emphasize our previous remarks concerning the distribution of fragment sizes. The assumption that one particle size is responsible for the wake phenomenon is almost certainly wrong. On the other hand, the fact that we can fit the observed and computed curves to within the error imposed by our ignorance of the diffusion

function shows that a more complex distribution function is not justified. Any other hypothetical distribution that contained an appreciable number of particles smaller than 10^{-6} grams would also produce a large intensity in the region of the dash. Our previous qualitative discovery that the majority of the luminosity is produced by fragments, would not be altered.

We shall first use our knowledge of the fragment size to study the effect of the meteor velocity on the presence of wake. Our observations (page 63) show that wake is more pronounced, in general, for lower velocity meteors. This observation is easily understood, in a qualitative fashion, if the wake is assumed to be composed of small fragments whose initial size is independent of the velocity of the meteor. The higher the velocity, the greater the deceleration imposed upon these particles. Then at any given lag, Δn, the particles from the faster meteors will have lost relatively more of their velocity than have the low velocity particles. As a consequence, their luminosity at this point will be relatively less and the wake not as pronounced.

This result has been quantitatively verified for hypothetical meteors at velocities of 15 and 35 km/sec, as well as for the previous case where v_o = 26.6 km/sec. For the case, v_o = 35 km/sec, we must make some allowance for the error caused by the false assumption that all particles producing the wake at some point are released from the meteor at essentially the same height. The computations

will show that the meteor will decrease in height by approximately β (1 scale height) before a particle can acquire a lag of $\Delta n = 0.5$. We cannot, then, use the same intensity-versus-lag relationship for the luminosities at the beginning and at the end of a break. Furthermore, we may no longer expect that the rate of fragmentation, $\dot{m}_p$, will remain constant over the time require ($n = 15$) for the first fragmented particle to be retarded by $\Delta n = 0.5$. In order to estimate how this rate will vary, we need not know the exact process by which particles fragment, but we may assume that the rate will be proportional to the area of the meteoroid. Since our calculations have been for the beginning of a meteor trail, where the area changes slowly, we may neglect the effect of changing area. Whether the detachment of the particles results from crushing due to the dynamic pressure (ρv^2), or to an energy transfer to the bonds which attach the fragment to the meteor (ρv^3), we should expect the mass loss to increase proportionally to the increase in the air density, ρ. The velocity change of the meteor between $n = 0$ and $n = 15$ will not exceed several percent and may be neglected. Thus, we may plausibly estimate that the mass loss would increase in these circumstances by a factor of e, the ratio of the densities at heights separated by a scale height. Actually, this choice of the mass loss may be considered to be dictated by

observation alone. To a good first approximation, the light curves of most meteors are predicted by the usual mass-loss and intensity equations, which are based on the assumption of atomic ablation from the meteoroid. Since the fragments themselves are ablated in a fairly short time and, indeed, produce most of their light in a very short time, the introduction of the intermediate step of fragmentation will not alter the general shape of the light curve if the fragmentation does not occur very much more rapidly than the ablation of the fragments.

Consequently, for the case of v_o = 35 km/sec we have computed the linear intensity versus lag curve (equation for the two initial conditions of ρ_o and 2.3 ρ_o with the mass losses of $\dot{m}_p$ and 2.3 $\dot{m}_p$, respectively. Intensity curves were drawn for both of these. We determined the intensity to be expected for the actual wake by setting the wake intensity in and near the dash equal to the intensity derived from particles detached from the meteor at the dash (n = 15), while the wake intensity in the break (Δn = 0.5) was set equal to the intensity derived from particles detached from the meteor at n = 0. For other values of n, a smooth curve was drawn, going in transition between these two extreme cases. The initial height, described by ρ_o, is the average beginning height for faint meteors of this velocity. Cos Z_R has been taken as

0.717, which corresponds to the observed value for the case at $v_o = 26.6$, computed previously.

For the case $v_o = 15$ km/sec, the change in height of the meteor is small over the time required for the particles to show an appreciable lag and the extensive corrections applied above were unnecessary. Also, the initial height chosen for this computation is the average beginning height for faint meteors of this velocity. Cos Z_R was taken as the same value as the one used for the case of $v_o = 35$ km/sec.

Computations for the case $v_o = 26.6$, have already been made in connection with the previous analysis of meteor No. 3567. These results apply to particles detached from a meteor at a point 3 km lower than the average beginning height of meteors of this velocity.

Figure 15 shows the expected intensity in arbitrary units in the course of one shutter cycle for the three cases. For comparison we have normalized these curves so that the total intensity in the dash, $-0.25 \leq \Delta n \leq 0.0$, is the same for all cases. It is interesting to note that the differences in velocities here have very little effect in changing the shape of the intensity curve in the dashes. Those differences that do exist are of the order of a few percent, and no attempt has been made to illustrate these departures from the mean dash curve displayed in Figure 15.

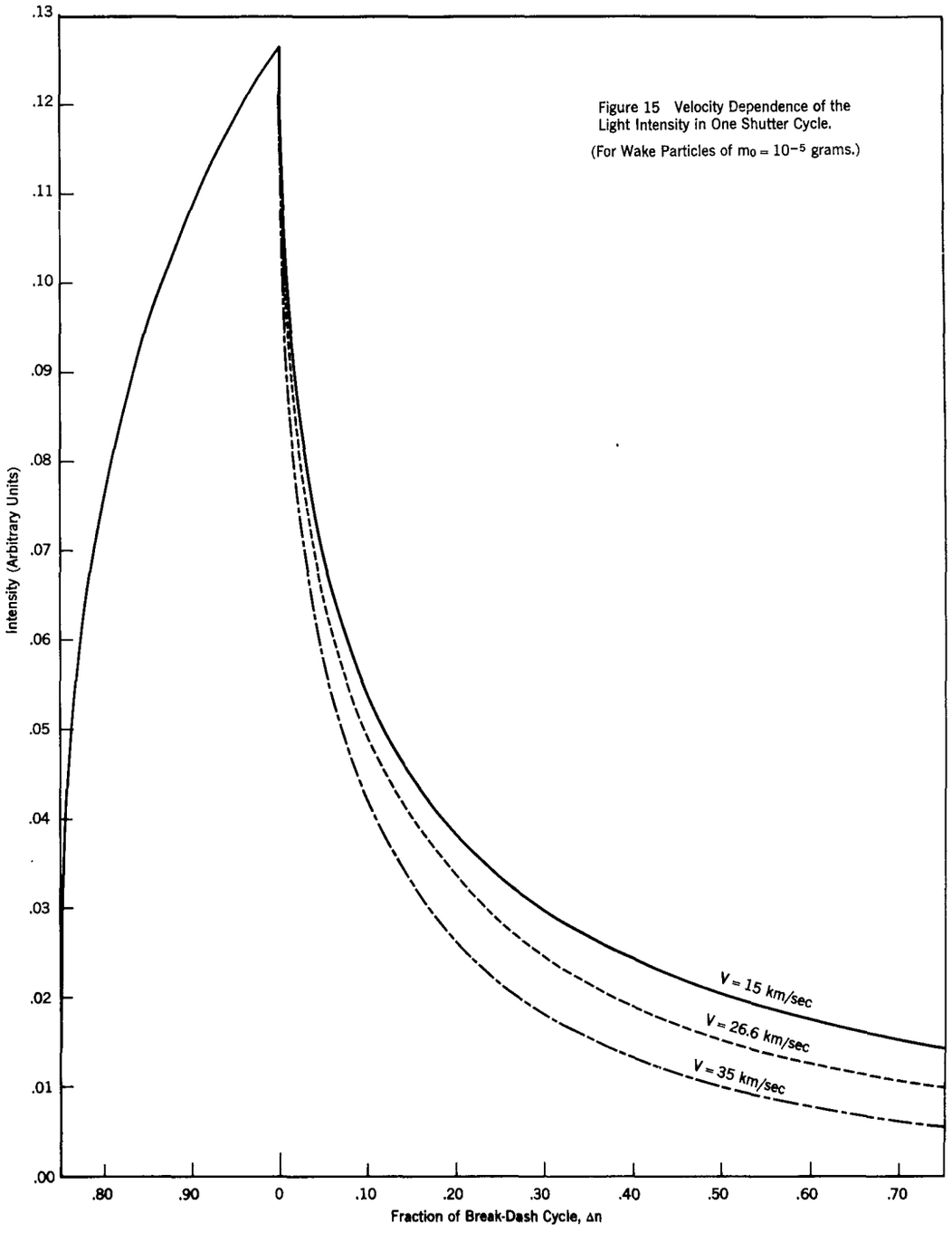

Figure 15 Velocity Dependence of the Light Intensity in One Shutter Cycle.

(For Wake Particles of $m_0 = 10^{-5}$ grams.)

It is clear from this figure that wake should be expected to be a low-velocity meteor phenomena, as observed. Three additional factors, not included in the calculations, modify the preceding results. Our observational data are entirely visual, and to make a fair comparison we should take into account the fact that the eye is capable of detecting a faint and long image as easily as it detects another image that is brighter but shorter. Since, in general, the faster meteors produce longer dashes, we should expect that this effect would partly overcome the ability of slower meteors to produce a visibly detectable luminosity in the wake.

On the other hand, we have compared the undiffused theoretical light curve and our observations are based on diffuse images. With this correction applied, the shorter images produced by the slower meteors will have the advantage that a greater portion of the dash luminosity is diffused into the break.* This factor will certainly outweigh the

*The lesser importance of diffusion on the dashes of high-velocity meteors can be easily seen on microdensitometer tracings of such trails. The tracings often show a dash profile on the same nature as the undiffused curve plotted in Figure 15. These dashes show a distinct maximum at the point $\Delta n = 0$, decreasing by as much as 0.5 magnitudes at the point $\Delta n = 0.75$. This confirms our supposition that much of the meteor luminosity results from small particles. Also, it demonstrates the power of the densitometer technique -- this change in intensity can not be detected by eye.

visibility argument and will increase the probability that wake may be detected for low-velocity meteors.

Finally, we have also seen that high-velocity meteors must persist for a far longer interval of time for wake to be detected. For example, if our hypothetical meteor of 35 km/sec velocity had had a lifetime of 10 dashes, little wake would have been observed, since even those particles that fragmented at the meteor's beginning would have been retarded only by an amount $\Delta n = 0.16$. On the other hand, a meteor of 15 km/sec under the same conditions would have wake particles at $\Delta n = 0.54$.

On this basis one would expect that the observed distinction in the velocity of wake-producing meteors would diminish if one were to observe brighter meteors of longer duration. Such is indeed the case: essentially all long meteors display wake, independently of their velocity. However, this fact may be explained just as easily in terms of the increased size, and consequent increased mass-loss and luminosity, of the longer meteors.

E. Terminal Blending

Continuous fragmentation of meteors wherein all or most of the luminosity arises from small particles offers a simple and satisfactory explanation of some examples of terminal blending. This elongation of the final dashes was reported by Jacchia (1954) to occur in approximately one-third

of the 137 long meteors analyzed. In these cases there was no good correlation with either velocity or brightness. Our own results show that this phenomenon does occur more frequently with low-velocity meteors.

The light curve of a meteor with blended dashes often shows no abrupt variations from that of a normal meteor, although the blended section itself is characterized by a nearly constant intensity, at variance with the ending of a normal meteor. Blending is most often seen, in faint meteors, for two or three dashes, but in extreme cases it has been visible for an estimated 50 dashes. More often than not, meteors that display a wake are not blended.

Let us consider a normal meteor, with no sharp discontinuities in the light curve, as it nears the end of its trajectory. If it has been fragmenting particles, we may or may not detect a wake, depending on its velocity and duration. At this point in the meteor's path, the rate of fragmentation will decrease rapidly due to the decrease in area and, as a consequence, the luminosity in the region of the dash will be reduced. However, the luminosity in the wake may be relatively high, since it results from the far larger number of particles that were fragmented when the meteor area was appreciably larger. When the luminosity due to smaller number of larger masses equals the larger number of smaller masses, wake and dash will be

indistinguishable and terminal blending will be present.

In those cases where terminal blending occurs suddenly without any previous wake, this approach appears to fail, or at least to require the very special case of wake becoming appreciable just as the meteor ends its trajectory. However, this explanation does overcome the difficulty of a previous suggestion in which it was assumed that the meteor suddenly crumbled near the end of its path, into many pieces of comparable size. Such an overall fragmenting would result in a burst of luminosity, which is not observed.

REFERENCES

Carrol, P. S., McCrosky, R. E., Wells, R. C., and Whipple, F. L. 1951 Harvard Reprint II-39, "Film Molding and Photographic Accessories for the Super-Schmidt Meteor Cameras"

Cook, A. F. and Millman, P. M. 1955 Ap. J. 121, 250, "Photometric Analysis of a Spectrum of a Perseid Meteor"

Cook, M. A., Eyring, H. and Thomas, R. N. 1951 A. J. 113, 475, "The Physical Theory of Meteors I. A Reaction-Rate Approach to the Rate of Mass Loss in Meteors"

de Jonge, J. H. K. 1954 Thesis, Harvard University, "On the Absolute Magnitudes of the A-Type Stars"

Hoffleit, D. 1933 Proc. Nat. Ac. Sci. 19, 212, "A Study of Meteor Light Curves"

Jacchia, L. G. 1949 Harvard Reprint II-31, "Photographic Meteor Phenomena and Theory"

_____ 1954 Status Report No. 7, Meteor Analysis Project at Harvard College Observatory

_____ 1955 Ap. J. 121, 521, "The Physical Theory of Meteors VIII. Fragmentation as a Cause of the Faint Meteor Anomaly"

Liller, W. and Whipple, F. L. 1954 "Rocket Exploration of the Upper Atmosphere," (Boyd and Seaton, Pergamon Press Ltd., London)

McCrosky, R. E. 1955 A. J. 60, 170 (abstract) "Fragmentation of Faint Meteors"

Millman, P. M. and Hoffleit, D. 1937 Har. Ann. 105, 601, "A Study of Meteor Photographs Taken Through a Rotating Shutter"

Millman, P. M. 1952 J. R. Astr. Soc. Can. 46, 121

_____ 1953 J. R. Astr. Soc. Can. 47, 217

Norton, A. P. 1946 "Norton's Star Atlas," p. 43, (Gall and Inglis, London)

REFERENCES (continued)

Olivier, C. P. 1925 "Meteors" (Williams and Wilkins, Baltimore)

Opik, E. 1933 Harvard Reprint 100 "Atomic Collisions and Radiation of Meteors"

Rinehart, J. S., Allen, W. A., and White, W. C. 1952 Jour. Ap. Phys. 23, 132, 198, 297, "Phenomena Associated with the Flight of Ultra Speed Pellets" (Parts I, II, and III)

Smith, Henry J. 1954 Ap. J. 119, 438, "The Physical Theory of Meteors V. The Masses of Meteor Flare Fragments"

"Tables of Sine, Cosine and Exponential Integrals" (W.P.A., 1940)

The Rocket Panel 1952 Phys. Rev. 88, 1027, "Pressures, Densities and Temperatures in the Upper Atmosphere"

Thomas, R. N. and Whipple, F. L. 1951 Ap. J. 114, 448, "The Physical Theory of Meteors II. Astroballistic Heat Transfer"

Thomas, R. N. 1952 Ap. J. 116, 203, "The Physical Theory of Meteors III. Conditions at the Meteor Surface"

Trowbridge, C. C. 1907 Ap. J. 26, 95

Whipple, F. L. 1939 Pop. Ast. 47, 419, "Upper Atmospheric Densities and Temperatures from Meteor Observations"

_____ 1950 Ap. J. 111, 375, "A Comet Model"

_____ 1951 Pop. Ast. 56, 144, "The Baker Super-Schmidt Meteor Cameras" (abstract)

_____ 1952 A. J. 57, 28, "On Meteor Masses and Densities" (abstract)

_____ 1953 Jour. of Meteorology 10, 390, "Winds in the Upper Atmosphere by Meteor Train Photography"

_____ 1954 A. J. 59, 201, "Photographic Meteor Orbits and Their Distribution in Space"

REFERENCES (continued)

Whipple, F. L. and Jacchia, L. G. (in press) Smithsonian Astrophysical Contribution, No. 1, "Reduction Methods for Photographic Meteors"

Wright, F. W., Jacchia, L. G. and Whipple, F. L. (in press) A. J. "Photographic α-Capricornid Meteors"

SUMMARY

The problem of meteor fragmentation is not a new one. Large meteorites have been observed to burst in flight and often a meteor fall will consist of a shower of bodies which are apparently due to the fracturing of a larger body.

However, our concern is not with the massive meteorites, but rather with small meteors whose maximum intensities range from $+3^{rd}$ to 0^{th} magnitude. An immense amount of material has been gathered on such objects within the past few years through the use of the new Baker Super-Schmidt meteor cameras.

Two of these instruments, separated by about 18 miles are used to photograph the same meteor. The cameras are equipped with rotating shutters that occult the meteor trail at known intervals. From such photographs, the intensity, height, velocity and deceleration of the meteor may be determined. Using the classical meteor theory, one may either (a) solve for the density of the atmosphere from the known deceleration or (b) assume the density to be known and determine those constants, occurring in the equations, for which we have only estimated values. In recent years, since the advent of the high altitude research rocket and the resultant increase in knowledge of the upper atmosphere, the meteor astronomer has tended to take the second approach.

Investigations by Whipple and by Jacchia have shown that the average meteor photographed in the Harvard program must be quite a different object from the meteorite. It seems entirely likely that the objects are of extremely low density -- less than that of water. Furthermore, the characteristics of the light curve of the meteor and of its dynamic behavior in the atmosphere can only be explained in terms of a fragmenting body.

Because of the high accuracy of measurement required to determine decelerations, only a small percentage of the photographic material has been reduced. We have developed a rapid graphical method of meteor trail reduction in order to acquire a greater body of data with which to study statistical aspects of the faint meteor phenomena. Reasonable estimates of the mean errors in the computed heights and velocities are, respectively, 3 percent and 5 percent.

Results for about 1000 meteors are included in this discussion. In general, these meteors represent a homogeneous group in terms of apparent maximum magnitude. Consequently, all meteors of a given velocity group are represented by the same mass. It is to be expected, on the basis of the present meteor theory, that such a group of meteors of the same velocity and mass should appear at the same height. It is found that the beginning heights for meteors with normal

light curves can be well represented by the relationship ρv^3 = constant where ρ is the atmospheric density and v is the meteor velocity.

Among the meteors studies, a group of low-velocity meteors comprising 13 percent of the total are peculiar in the sense that they display an abrupt rise of light at the beginning of the trail. A typical meteor of this group will rise from below the plate limit to 1 magnitude above in less than $\frac{1}{60}$ sec. The shutter breaks often become invisible at the end of the trajectory (terminal blending). Both of these phenomena can be explained by a sudden increase of the effective surface area of the meteoroid by fragmentation into a number of smaller pieces. The differential deceleration of fragments of different sizes cause the meteoroid to spread along the trail and obscure the shutter breaks.

Meteors of this group do not obey the ρv^3 = constant law for beginning points. However, the point at which the burst takes place can be described in terms of a constant value of the dynamic pressure, $\rho v^2 = 2.5 \cdot 10^4$ dynes/sq cm (0.02 atmospheres). Quite likely we have here a measure of the weak crushing strength of meteoritic material.

The height corresponding to the observed value of ρv^3 is greater, at all meteor velocities, than the height corresponding to the observed ρv^2 value. Consequently,

if the above hypothesis is correct we should expect to find occasionally a high-velocity meteor that first appears normally at the proper value of ρv^3 and then shows a fragmentation after its trajectory has carried it into the range where crushing may take place. In 1949, Jacchia reported 7 examples of high-velocity meteors that displayed an abrupt increase in luminosity some time after their appearance. The average value of ρv^2 at the point of discontinuity of the light curve agrees with the value obtained for those low-velocity meteors of this study which obey the ρv^2 law.

The meteor wake has also been studied in some detail. This phenomenon is characterized by a considerable amount of luminosity in the shutter breaks of the meteor trail. A study of those meteors reduced by the graphical method shows that wake occurs predominately in low-velocity meteors. We have also been able to show, conclusively, that the persistent trains are produced almost entirely by meteors of high velocity. Thus, it appears to be almost a certainty that we must require some new process to form the wake. Jacchia's concept of the continuous fragmentation of meteors offers an obvious starting point.

We assume that small particles are detached from the meteoroid and decelerate with respect to this parent body, thus causing the luminosity of the meteor to extend over a considerable distance at any given instant.

Such an assumption is sufficient to reproduce the observed wake but also necessitates that a large fraction of the light in the meteor be derived from the fragments and not the meteoroid directly. This is consistent with the observed values of the ablation constant, σ and with our observations showing the wake to be most noticeable in low-velocity meteors.